



The Abdus Salam
International Centre for Theoretical Physics

United Nations
Educational, Scientific
and Cultural Organization

International Atomic
Energy Agency

H4.SMR/1775-16

**"8th Workshop on Three-Dimensional Modelling of
Seismic Waves Generation, Propagation and their Inversion"**

25 September - 7 October 2006

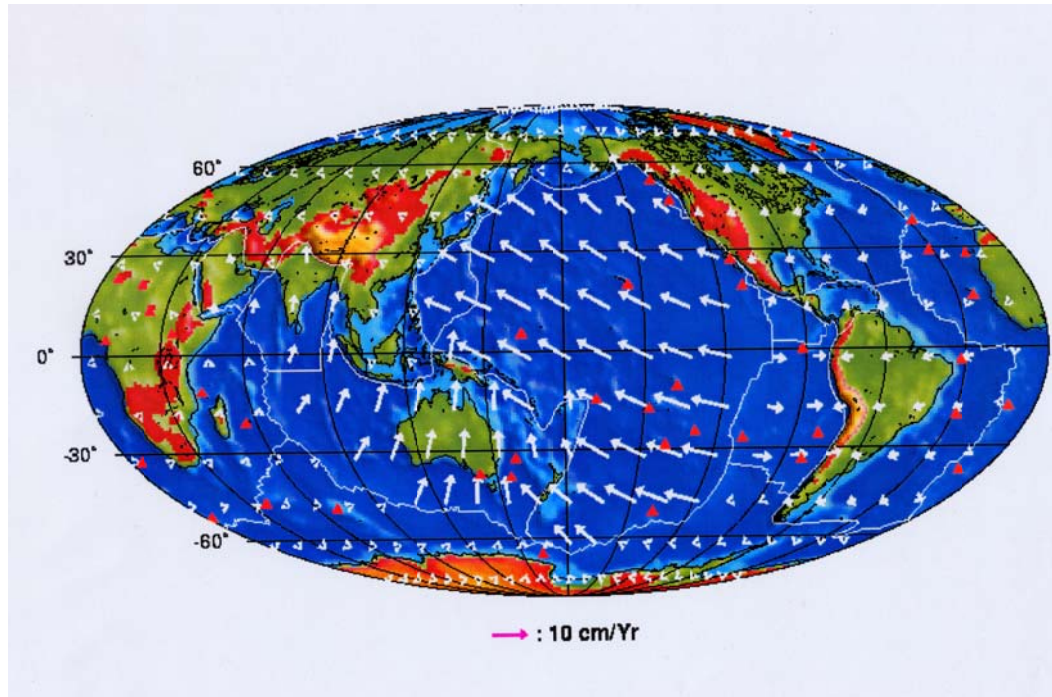
Surface Waves and Upper Mantle Anisotropy - II

Jean-Paul Montagner

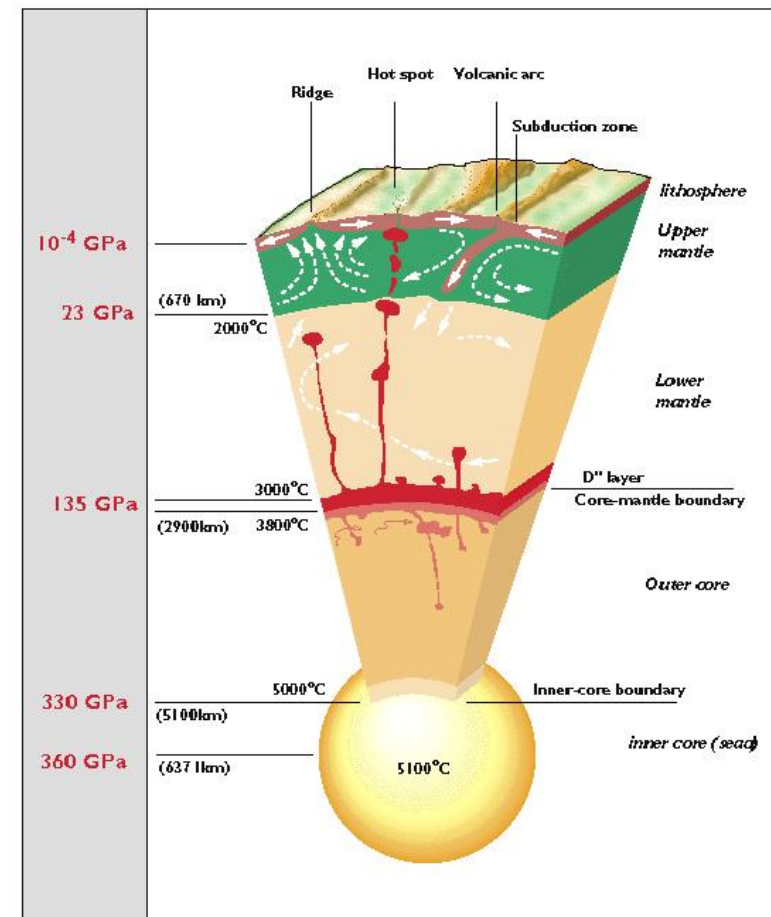
**Dept. Sismologie
I.P.G. Paris
France**

Structure of the Earth

Plate tectonics



Mantle Convection



Tomographic Technique

■ Forward Problem: Theory $\mathbf{d}=\mathbf{g}(\mathbf{p})$

\mathbf{d} data space, \mathbf{p} parameter space

- Reference Earth model \mathbf{p}_0 :

$$\mathbf{d}_0 = \mathbf{g}(\mathbf{p}_0)$$

- Kernels $\partial\mathbf{g}/\partial\mathbf{p}$

- \mathbf{C}_d function (or matrix) of covariance of data

■ Inverse Problem: $\mathbf{p}-\mathbf{p}_0 = \mathbf{g}^{-1} (\mathbf{d}-\mathbf{d}_0)$

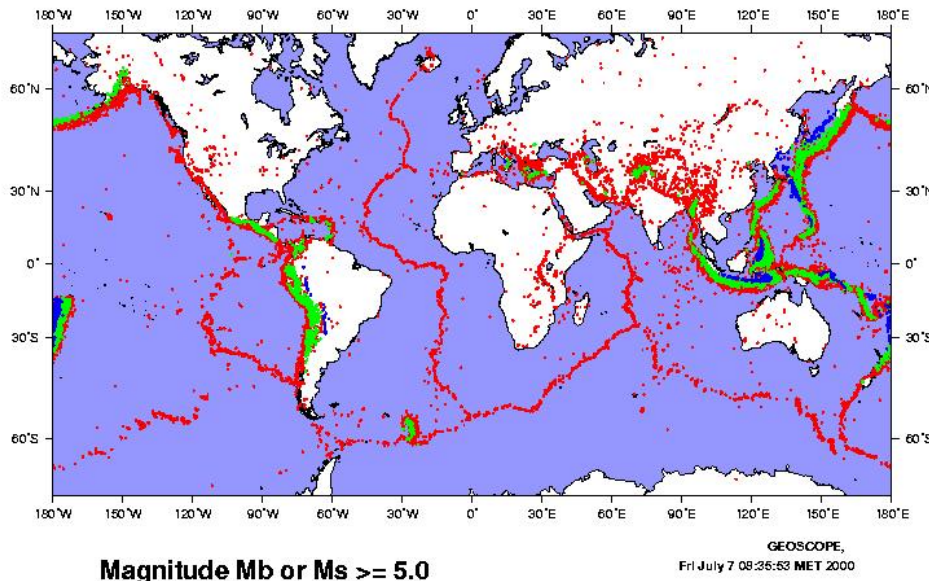
- \mathbf{C}_{p0} a priori Covariance function of parameters

- \mathbf{C}_{pf} a posteriori Covariance function of parameters

- R Resolution



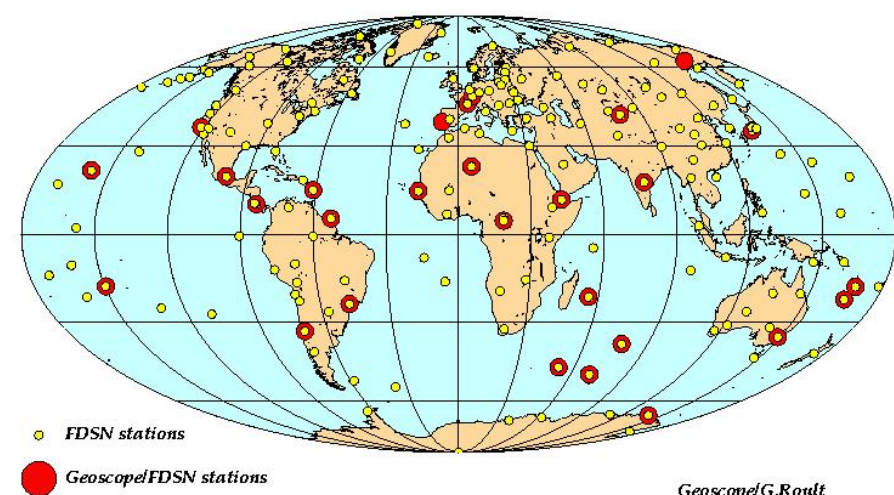
Global seismicity 1928-1999



Receivers

Seismic sources

GEOscope stations and FDSN stations

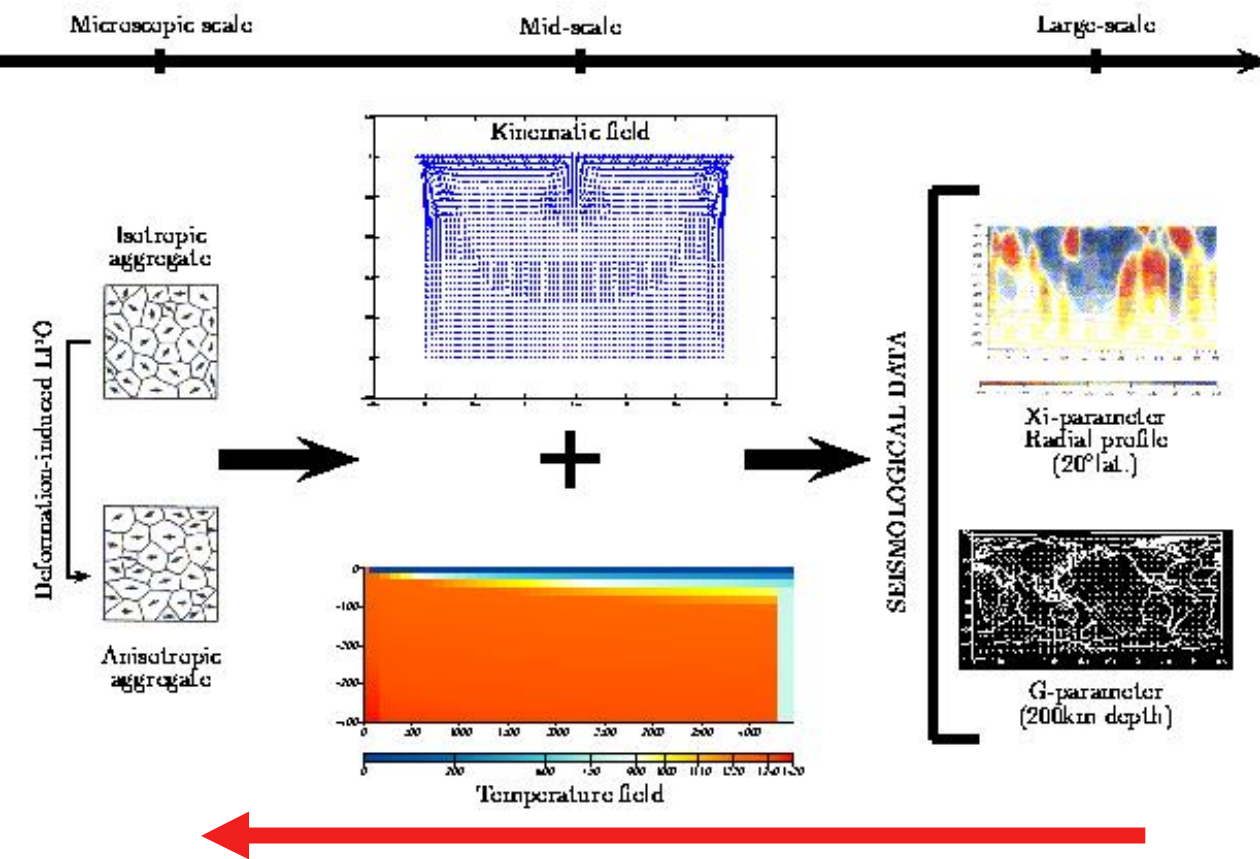




Importance of seismic anisotropy

ANISOTROPY is the Rule not the Exception

Seismic Anisotropy is present at all scales

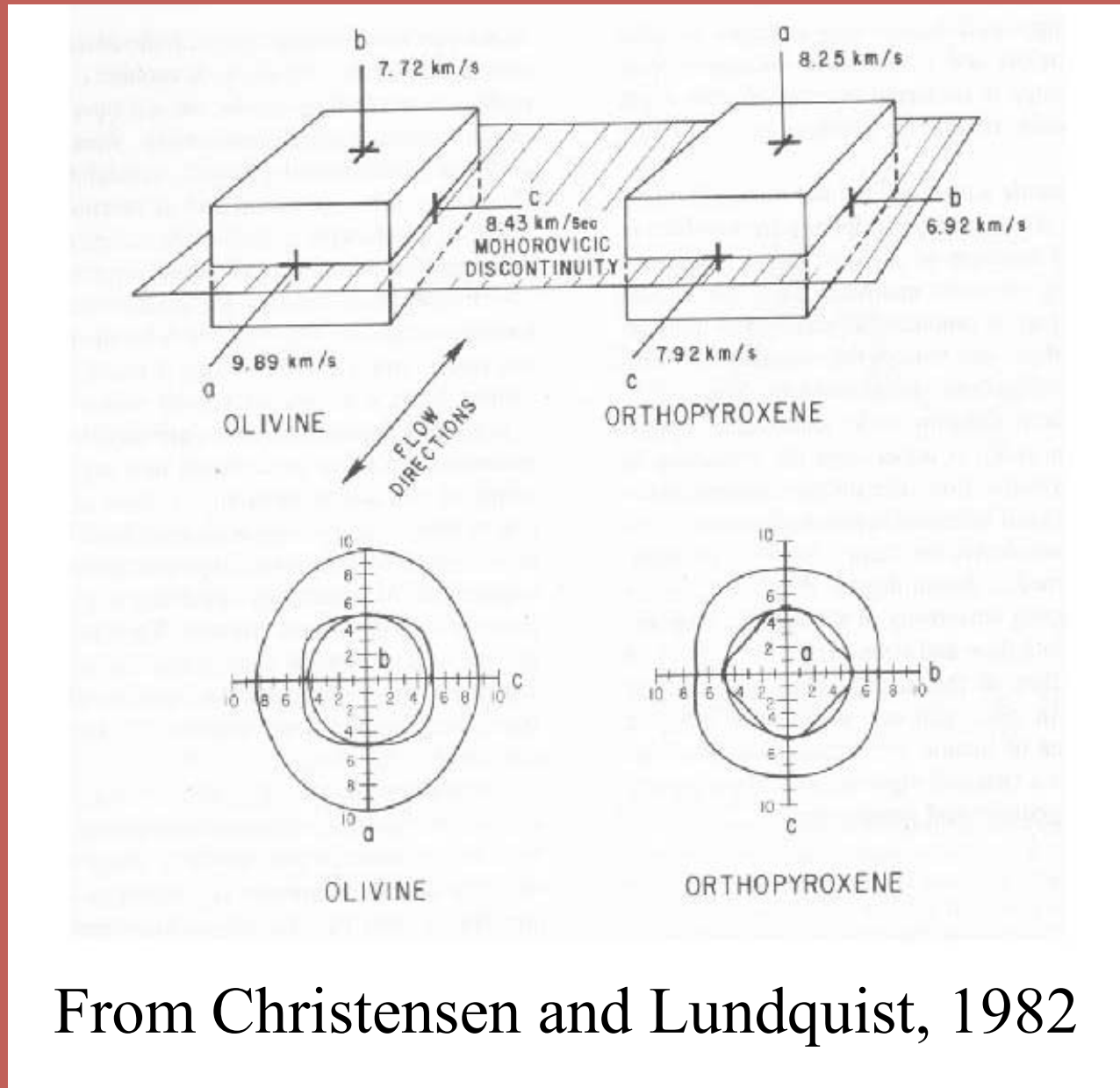


Mineralogical
composition

Mapping
Convection

(Montagner and Guillot, 2001)

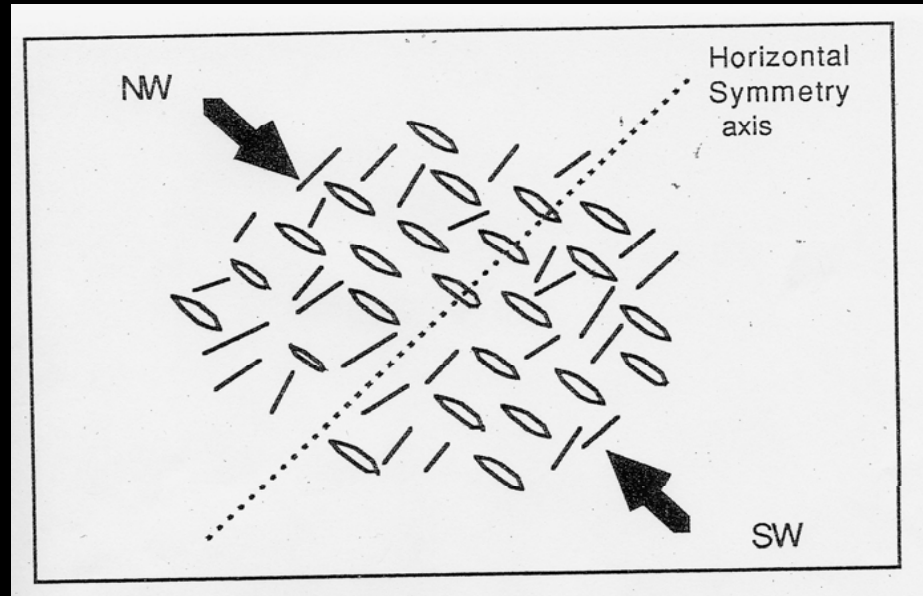
L.P.O. Lattice Preferred Orientation



From Christensen and Lundquist, 1982

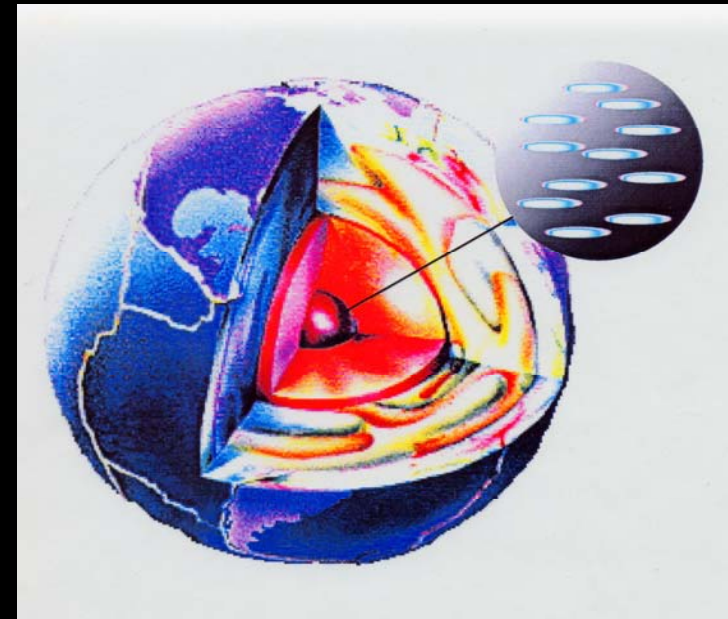
Cracks, fluid inclusions

Crust



(Babuska and Cara, 1991)

Inner core



(Singh et al., 2001)

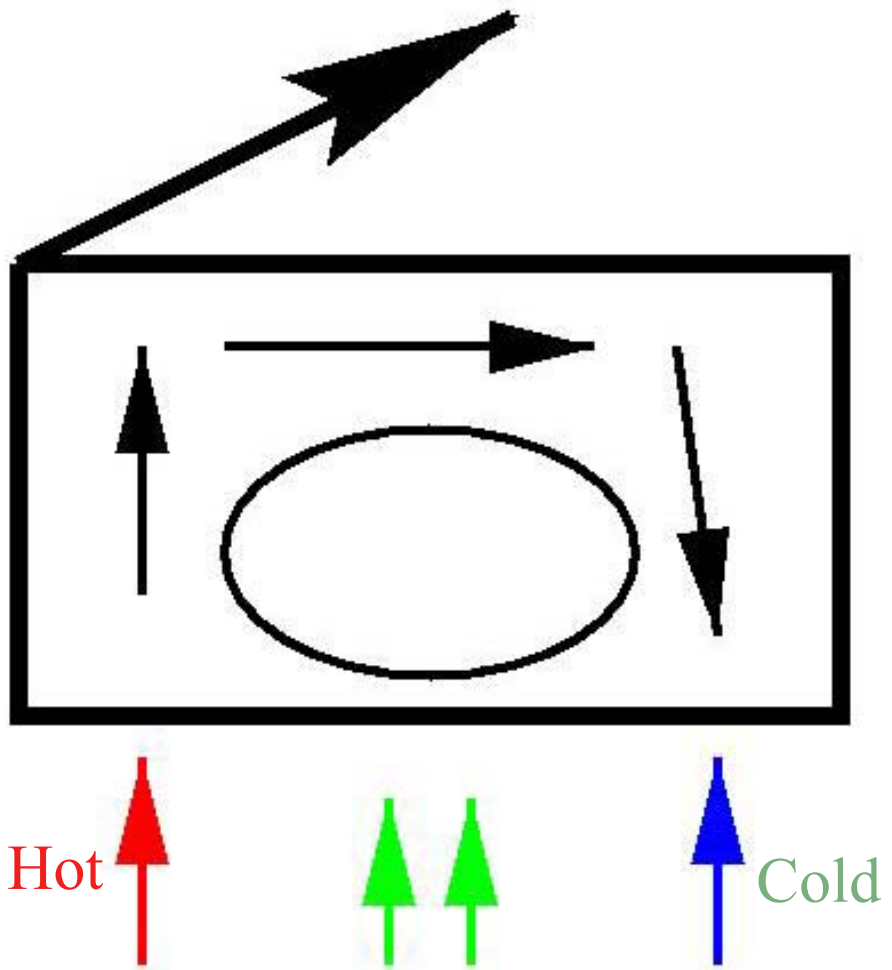


Importance of seismic anisotropy ANISOTROPY is the Rule not the Exception

Anisotropy is present at all scales

- From microscopic scale up to macroscopic scale
- Efficient mechanisms of alignment (L.P.O.: lattice preferred orientation S.P.O.: shape preferred orientation; fine layering)

Montagner & Guillot, 2001



$\Delta\alpha$ Effect of Mineral Orientation

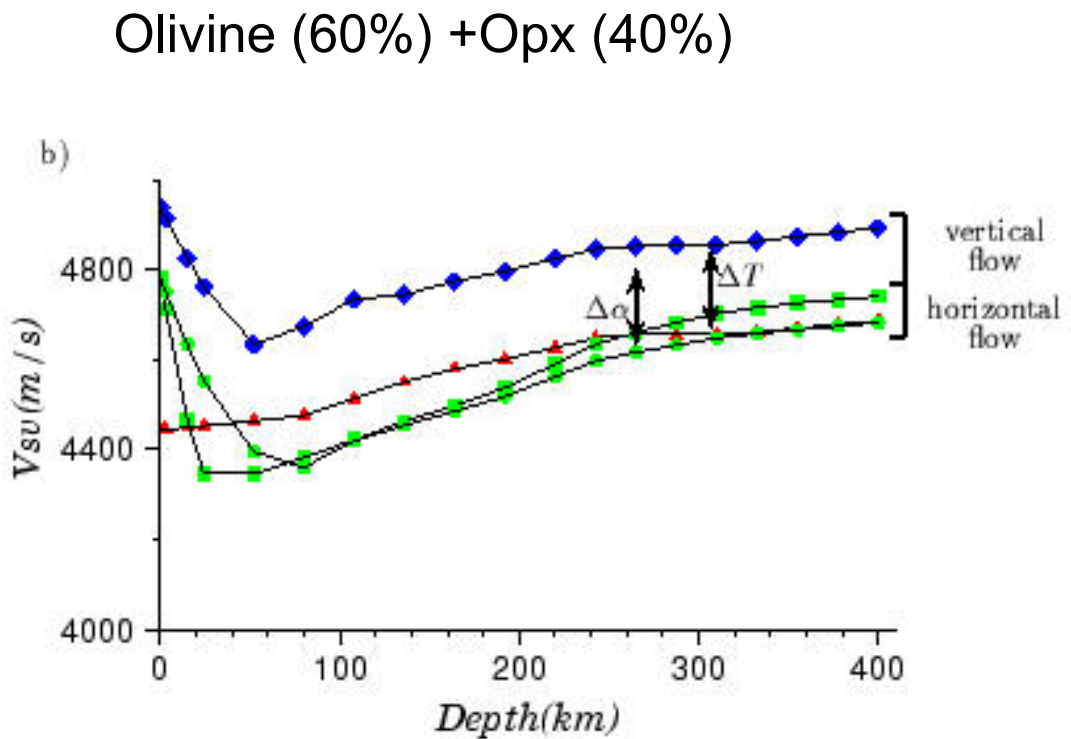
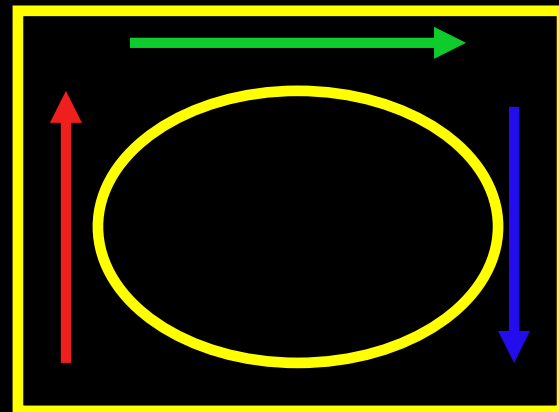
ΔT Effect of Temperature Heterogeneities



$\Delta\alpha$: Anisotropy Effect

ΔT : Temperature Effect

$$\Delta\alpha \approx \Delta T$$



Montagner & Guillot, 2002



Importance of seismic anisotropy
ANISOTROPY is the Rule not the Exception



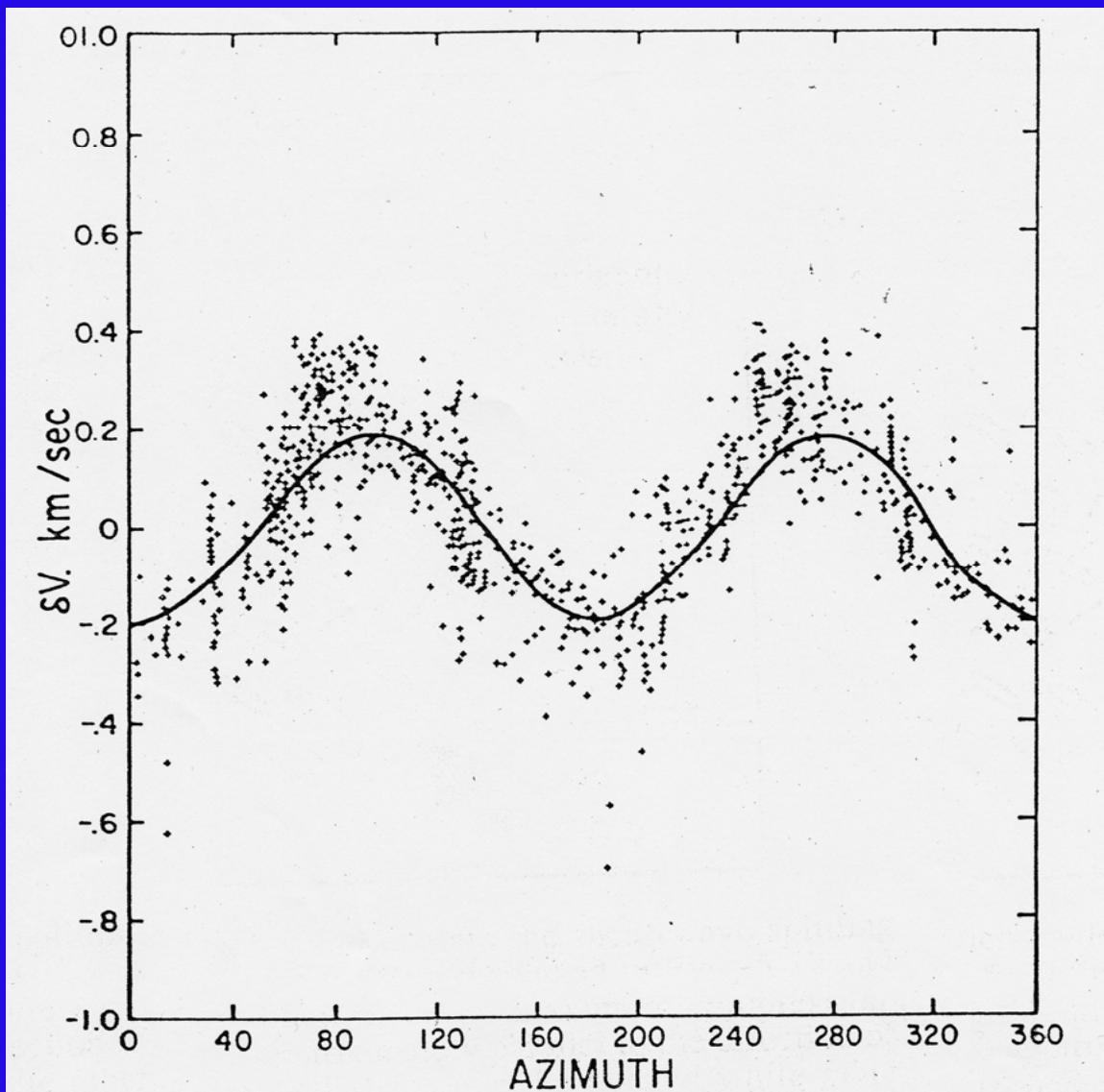
Anisotropy is present at all scales

- from microscopic scale to macroscopic scale
- Efficient mechanisms of alignment
(L.P.O.: lattice preferred orientation
S.P.O.: shape preferred orientation; fine layering)

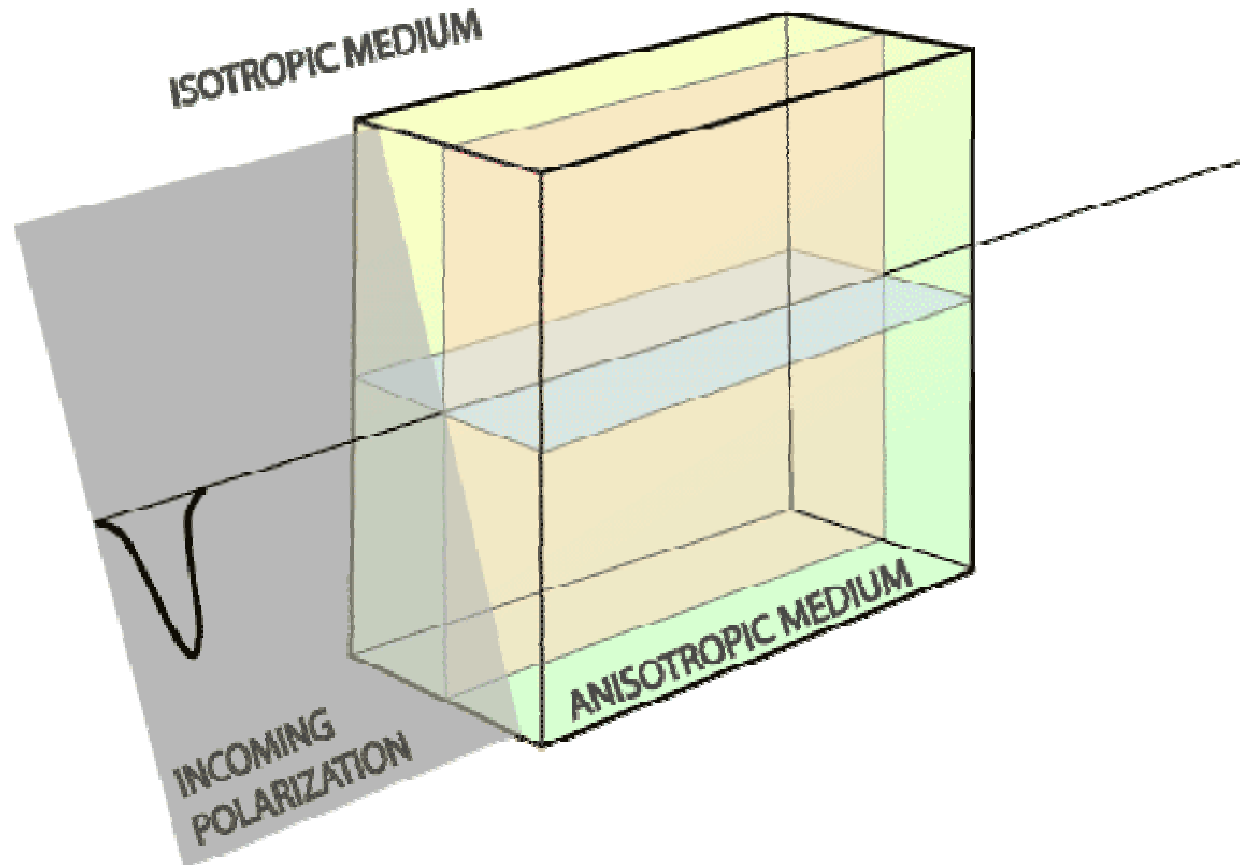
Anisotropy is observed on different kinds
of seismic waves

- Body waves (Pn; S-wave splitting)
- Surface waves (Rayleigh-Love discrepancy,
azimuthal anisotropy)

Pn- velocities

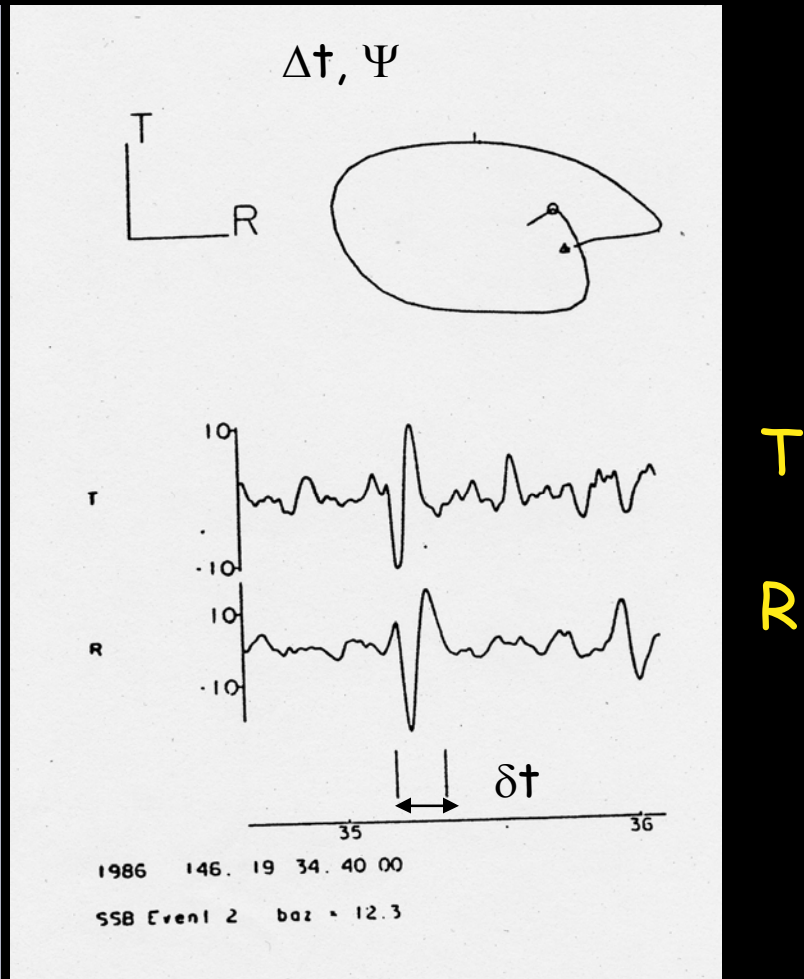
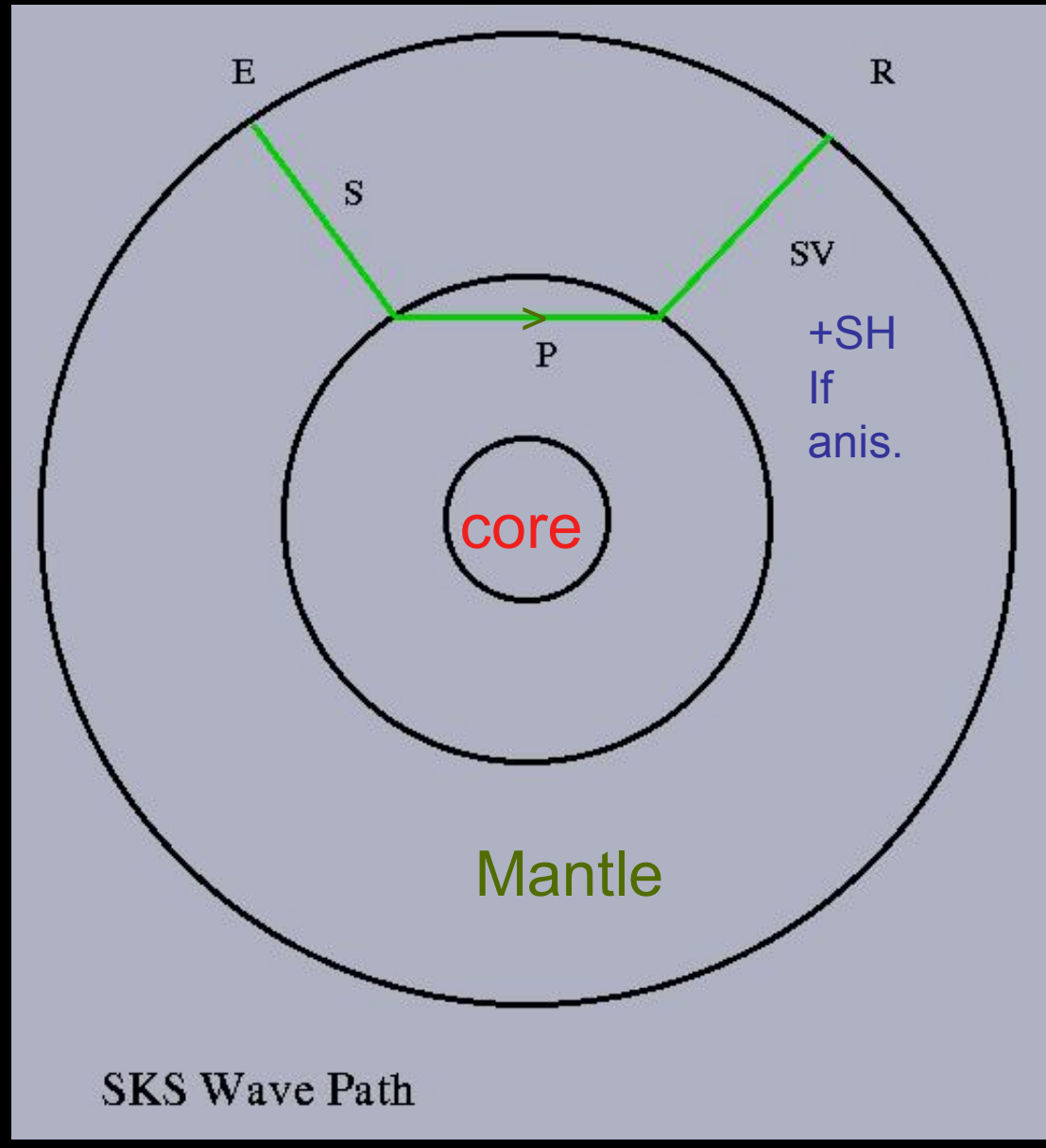


Shear Wave Splitting (Birefringence)



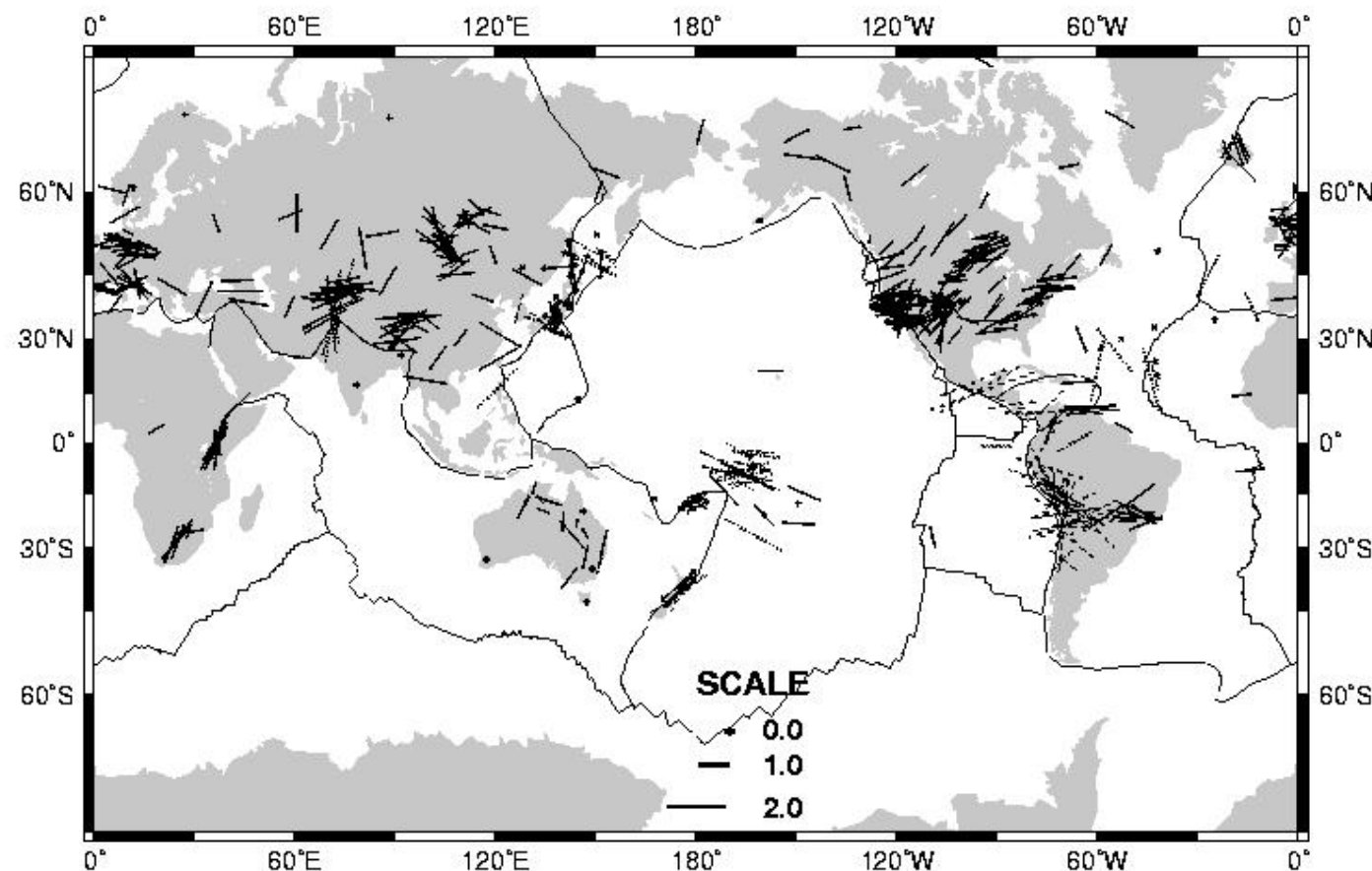
Animation courtesy of Ed Garnero

SKS- Splitting



Vinnik et al., 1989

Compilation of S-wave splitting measurements



Savage, Rev. Geophys., 1999



SURFACE WAVES



Importance of seismic anisotropy ANISOTROPY is the Rule not the Exception



Anisotropy is present at all scales

- from microscopic scale to macroscopic scale
- Efficient mechanisms of alignment
(L.P.O.: lattice preferred orientation
S.P.O.: shape preferred orientation; fine layering)

Anisotropy is observed on different kinds of seismic waves

- Body waves (Pn; S-wave splitting)
- Surface waves (Rayleigh-Love discrepancy, azimuthal anisotropy)

ANISOTROPY REFLECTS AN INNER ORGANIZATION

ANISOTROPY IS NOT A SECOND ORDER EFFECT

Effect of anisotropy on surface waves

Effect on eigenfrequency for multiplet $k=\{n,l,m\}$

$$\frac{\delta\omega_k}{\omega_k} = \frac{\int_{\Omega} \varepsilon_{ij}^* \delta C_{ijkl} \varepsilon_{kl} d\Omega}{\int_{\Omega} \rho_0 u_r^* u_r d\Omega} = \nabla V|_k$$

ε strain tensor, u displacement, δC_{ijkl} elastic tensor perturbation

Phase velocity perturbation $V(T,\theta,\phi,\Psi)$ at point $r(\theta,\phi)$ (Smith&Dahlen, 1973)

$$\begin{aligned} \delta V(T,\theta,\phi,\Psi)/V &= \alpha_0(T,\theta,\phi) + \alpha_1(T,\theta,\phi)\cos 2\Psi + \alpha_2(T,\theta,\phi)\sin 2\Psi \\ &\quad + \alpha_3(T,\theta,\phi)\cos 4\Psi + \alpha_4(T,\theta,\phi)\sin 4\Psi \end{aligned}$$

Ψ Azimuth (angle between North and wave vector)

The first order perturbation in Love wave phase velocity $\delta C_L(k, \Psi)$ can be expressed as:

$$\delta C_L(k, \Psi) = \frac{1}{2C_{0L}(k)} [L_1(k) + L_2(k)\cos 2\Psi + L_3(k)\sin 2\Psi + L_4(k)\cos 4\Psi + L_5(k)\sin 4\Psi]$$

where

$$\begin{aligned}
 L_0(k) &= \int_0^\infty \rho W^2 dz \\
 \text{OP} \leftarrow L_1(k) &= \frac{1}{L_0} \int_0^\infty (W^2 dN + \frac{W'^2}{k^2} dL) dz \\
 \text{2\Psi} \leftarrow \begin{cases} L_2(k) = \frac{1}{L_0} \int_0^\infty -G_c(\frac{W'^2}{k^2}) dz \\ L_3(k) = \frac{1}{L_0} \int_0^\infty -G_s(\frac{W'^2}{k^2}) dz \end{cases} \\
 \text{4\Psi} \leftarrow \begin{cases} L_4(k) = \frac{1}{L_0} \int_0^\infty -E_c \cdot W^2 dz \\ L_5(k) = \frac{1}{L_0} \int_0^\infty -E_s \cdot W^2 dz \end{cases}
 \end{aligned}$$

The same procedure holds for Rayleigh waves, starting from the displacement given previously.

$$\delta C_R(k, \Psi) = \frac{1}{2C_{0R}(k)} [R_1(k) + R_2(k)\cos 2\Psi + R_3(k)\sin 2\Psi + R_4(k)\cos 4\Psi + R_5(k)\sin 4\Psi]$$

where

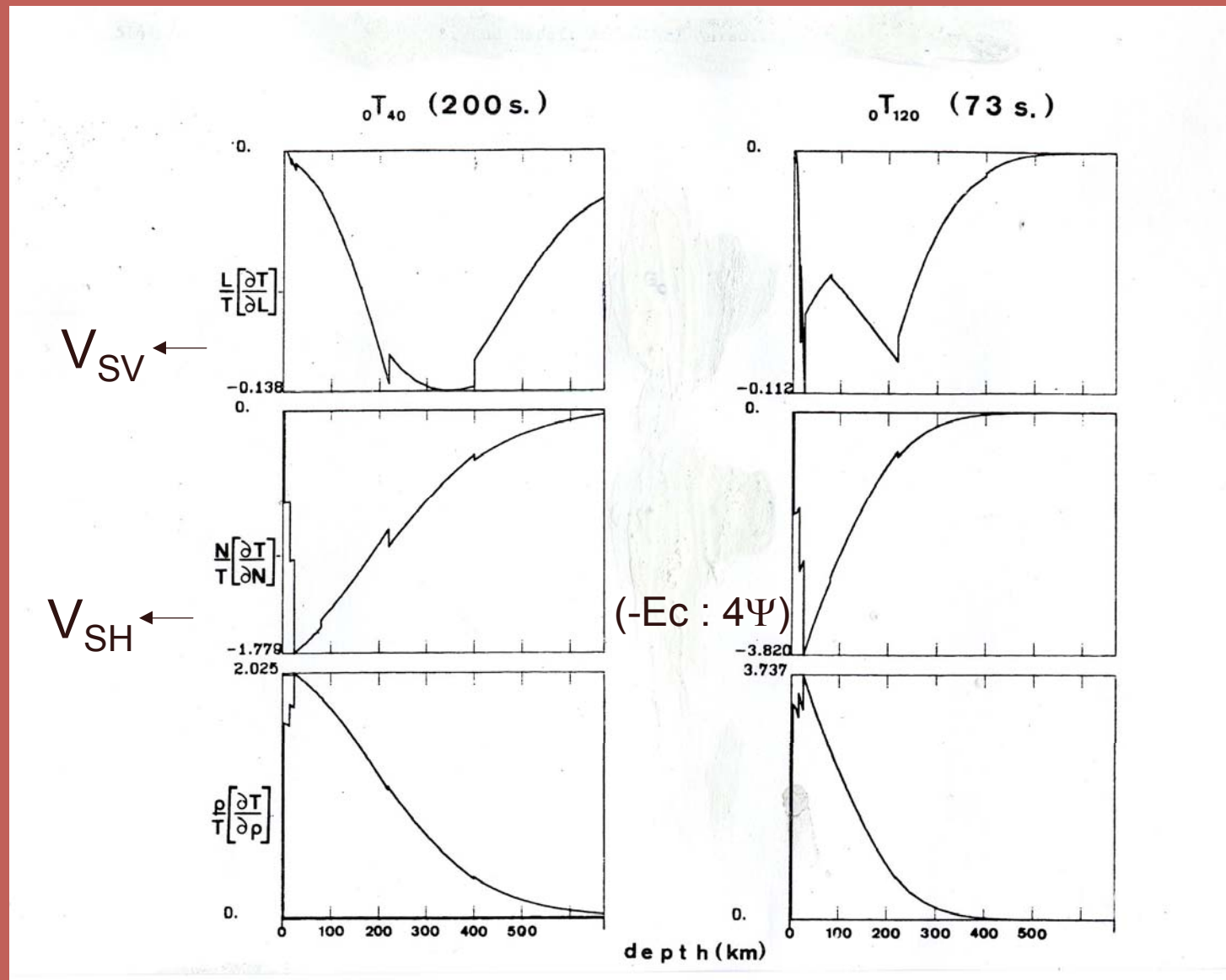
$$\begin{aligned} R_0(k) &= \int_0^\infty \rho(U^2 + V^2)dz \\ R_1(k) &= \frac{1}{R_0} \int_0^\infty [V^2 dA + \frac{U'^2}{k^2} dC + \frac{2U'V}{k} dF + (\frac{V'}{k} - U)^2 dL] dz \\ R_2(k) &= \frac{1}{R_0} \int_0^\infty [V^2 \cdot B_c + \frac{2U'V}{k} \cdot H_c + (\frac{V'}{k} - U)^2 G_c] dz \\ R_3(k) &= \frac{1}{R_0} \int_0^\infty [V^2 \cdot B_s + \frac{2U'V}{k} \cdot H_s + (\frac{V'}{k} - U)^2 G_s] dz \\ R_4(k) &= \frac{1}{R_0} \int_0^\infty E_c \cdot V^2 dz \\ R_5(k) &= \frac{1}{R_0} \int_0^\infty E_s \cdot V^2 dz \end{aligned}$$

The 13 depth-functions $A, C, F, L, N, B_c, B_s, H_c, H_s, G_c, G_s, E_c, E_s$ are linear combinations of the elastic coefficients C_{ij} and are explicitly given as follows:

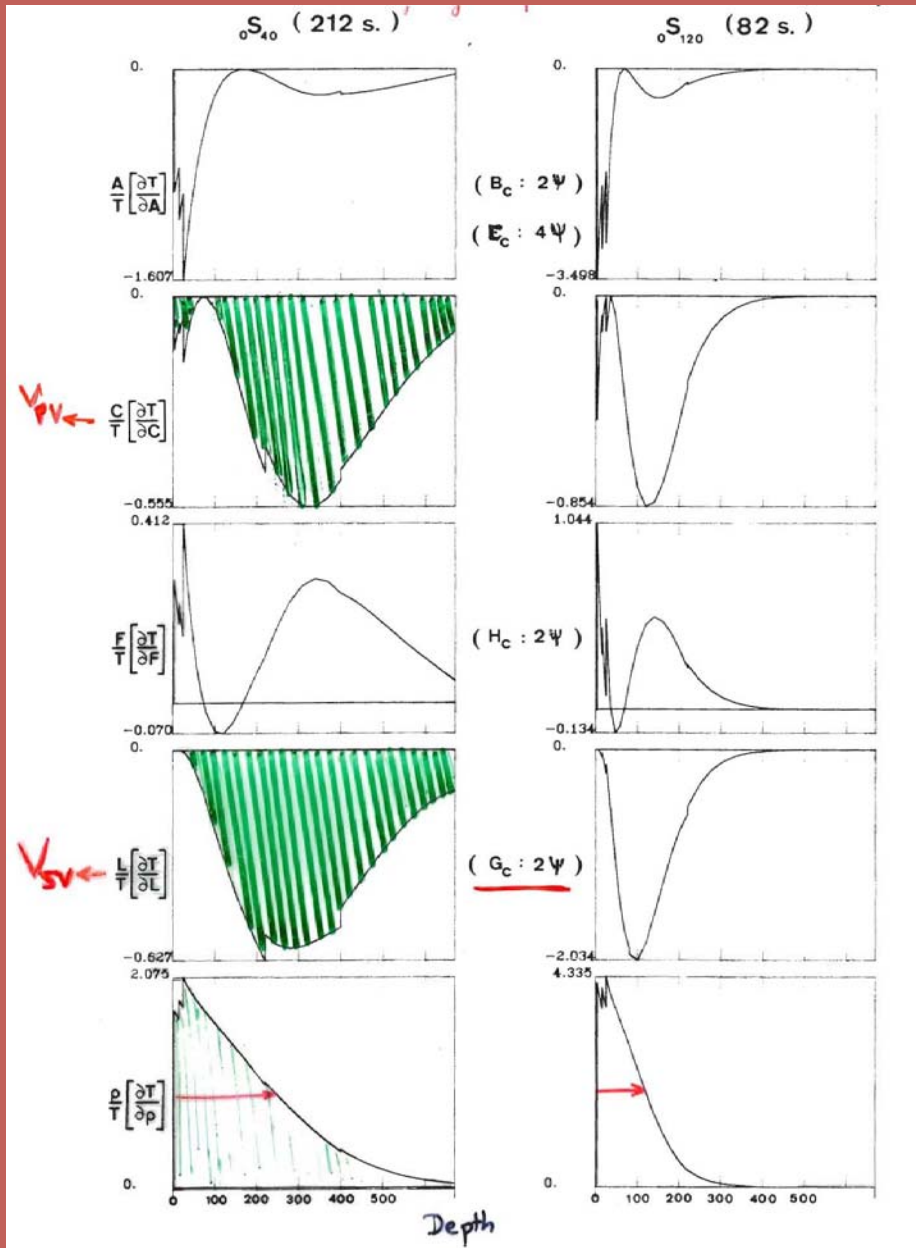
Table 1: Calculation of the various $c_{ij}\epsilon_i\epsilon_j$ for Love waves
 $\alpha = \cos\Psi; \beta = \sin\Psi$

| n | ij | $c_{ij}\epsilon_i\epsilon_j$ |
|---|----|---|
| 1 | 11 | $c_{11}\alpha^2\beta^2.k^2W^2$ |
| 1 | 22 | $c_{22}\alpha^2\beta^2.k^2W^2$ |
| 1 | 33 | 0 |
| 2 | 12 | $-c_{12}\alpha^2\beta^2.k^2W^2$ |
| 2 | 13 | 0 |
| 2 | 23 | 0 |
| 2 | 24 | |
| 4 | 14 | $c_{14}(-i\alpha^2\beta).\frac{kWW'}{2}$ |
| 4 | 15 | $c_{15}(i\alpha^2\beta).\frac{kWW'}{2}$ |
| 4 | 16 | $c_{16}(-\alpha\beta)(\alpha^2 - \beta^2).\frac{k^2W^2}{2}$ |
| 4 | 24 | $c_{24}(-i\alpha^2\beta).\frac{kWW'}{2}$ |
| 4 | 25 | $c_{25}(-i\alpha\beta^2).\frac{kWW'}{2}$ |
| 4 | 26 | $c_{26}(\alpha\beta)(\alpha^2 - \beta^2).\frac{k^2W^2}{2}$ |
| 4 | 34 | 0 |
| 4 | 35 | 0 |
| 4 | 36 | 0 |
| 4 | 44 | $c_{44}\alpha^2.\frac{W'^2}{4}$ |
| 8 | 45 | $c_{45}(-\alpha\beta).\frac{W'^2}{4}$ |
| 8 | 46 | $c_{46}(-i\alpha)(\alpha^2 - \beta^2).\frac{kWW'}{2}$ |
| 4 | 55 | $c_{55}\beta^2.\frac{W'^2}{4}$ |
| 8 | 56 | $c_{56}(i\beta)(\alpha^2 - \beta^2).\frac{kWW'}{2}$ |
| 4 | 66 | $c_{66}(\alpha^2 - \beta^2).\frac{k^2W^2}{4}$ |

Love wave partial derivatives



Rayleigh wave partial derivatives



13 parameters

| | | | |
|------------|--|--|---------------------|
| 0\Psi term | $A = \frac{3}{8}(C_{11} + C_{22}) + \frac{1}{4}C_{12} + \frac{1}{2}C_{66}$ | $\rightarrow V_{PH}$ | $\leftarrow V_{PV}$ |
| | $C = C_{33}$ | $\rightarrow V_{PV}$ | |
| | $F = \frac{1}{2}(C_{13} + C_{23})$ | | |
| | $L = \frac{1}{2}(C_{44} + C_{66})$ | $\rightarrow V_{SV}$ | $\leftarrow V_{SH}$ |
| | $N = \frac{1}{8}(C_{11} + C_{22}) - \frac{1}{4}C_{12} + \frac{1}{2}C_{66}$ | $\rightarrow V_{SH}$ | |
| | cos | sin | |
| 2\Psi term | $B_c = \frac{1}{2}(C_{11} - C_{22})$ | $B_s = C_{16} + c_{26} \rightarrow B$ | \leftarrow |
| | $G_c = \frac{1}{2}(C_{55} - C_{44})$ | $G_s = C_{54} \rightarrow G$ | \leftarrow |
| | $H_c = \frac{1}{2}(C_{13} - C_{23})$ | $H_s = C_{36} \rightarrow H$ | |
| 4\Psi term | $E_c = \frac{1}{8}(C_{11} + C_{22}) - \frac{1}{4}C_{12} - \frac{1}{2}C_{66}$ | $E_s = \frac{1}{2}(C_{16} - C_{26}) \rightarrow E$ | |

Transversely
Isotropic
Medium
With vertical
Symmetry axis

Isotropic medium: 2 parameters
 VTI: 5 parameters (A, C, F, L, N)
 + 8 (from surface waves)

Montagner and Nataf, 1986

13 parameters

- Best Resolved parameters for Surface Waves

$L = \rho V_{SV}^2$ Isotropic part of V_{SV} .

$\xi = \frac{N}{L} = \frac{V_{SH}^2}{V_{SV}^2}$ Radial Anisotropy.

G, Ψ_G Azimuthal Anisotropy of V_{SV} , also related to SKS splitting
(when horizontal symmetry axis).

+ a priori information (from mineralogy, ...)

- Body Waves (*Crampin, 1984*)

$$\rho V_{qSV}^2 = L + G_e \cos 2\Psi + G_s \sin 2\Psi$$

$$\rho V_{qSH}^2 = N - E_e \cos 4\Psi - E_s \sin 4\Psi$$

Geodynamic Interpretation

S- Velocity

Radial Anisotropy

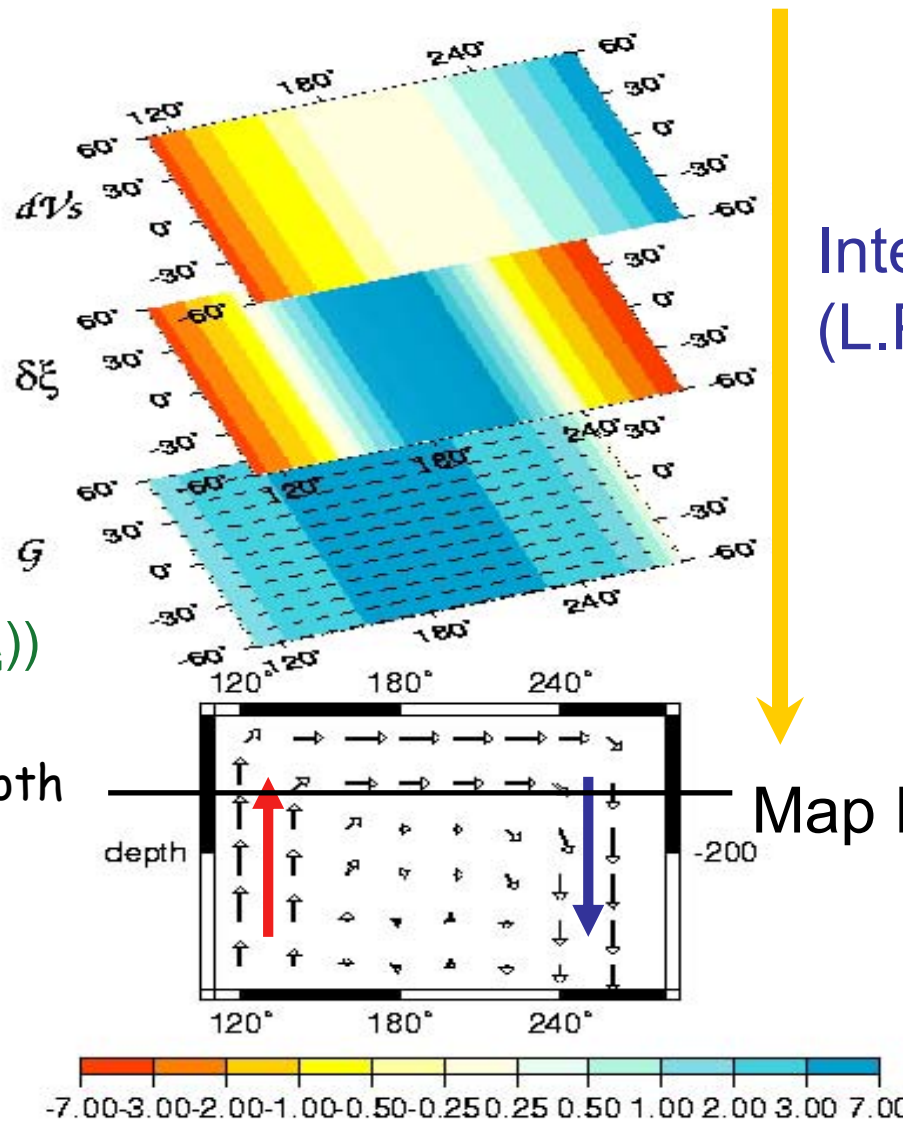
$$\xi = (V_{SH}^2 - V_{SV}^2) / V_{SV}^2$$

Azimuthal Anisotropy

$$V_{SV} \approx V_{SV0} + \frac{1}{2} G \cos(2(\Psi - \Psi_G))$$

At a given depth

Convective cell: anisotropic parameters

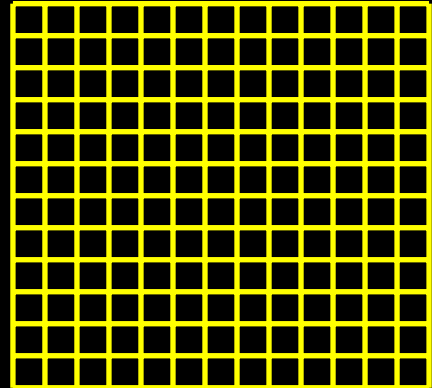


Interpretation
(L.P.O.)

Map Flow

2 D tomography: N cells

Isotropic Inversion:



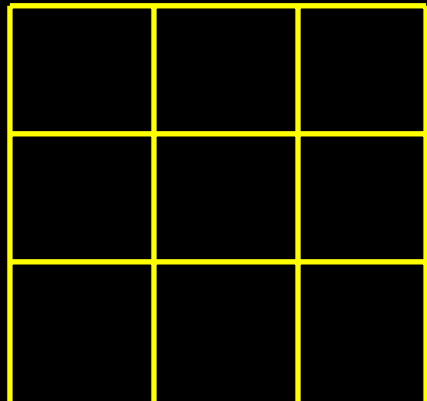
N independent parameters

0- Ψ term

VR1

Variance reduction

Anisotropic inversion



$$3N' = N$$

0+2 Ψ term

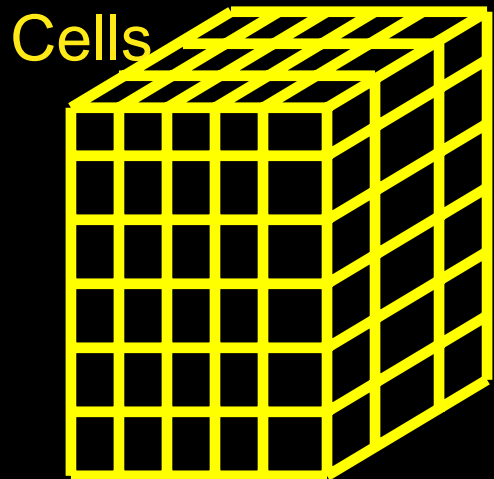
VR2

VR2 > VR1 => the anisotropic model can be simpler than the isotropic model

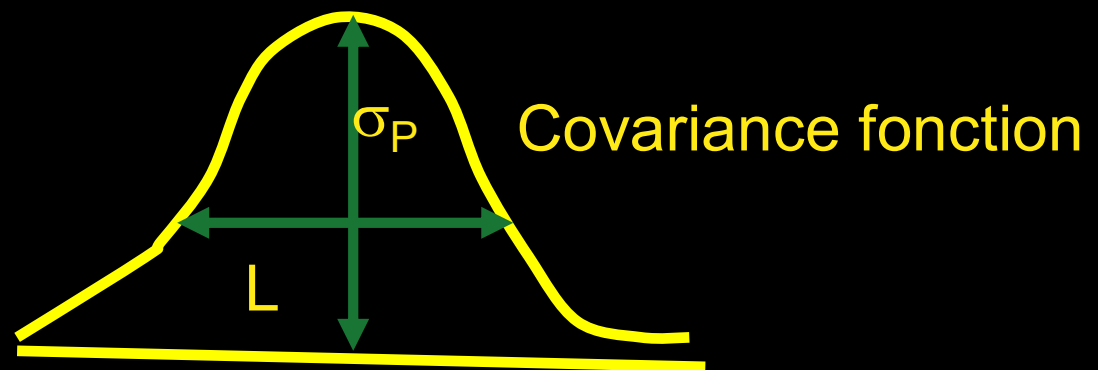
Parameter Space

Physical parameters: $\rho + 13$ physical parameters

Geographical parameterization: $\mathbf{p}(r, \theta, \phi)$

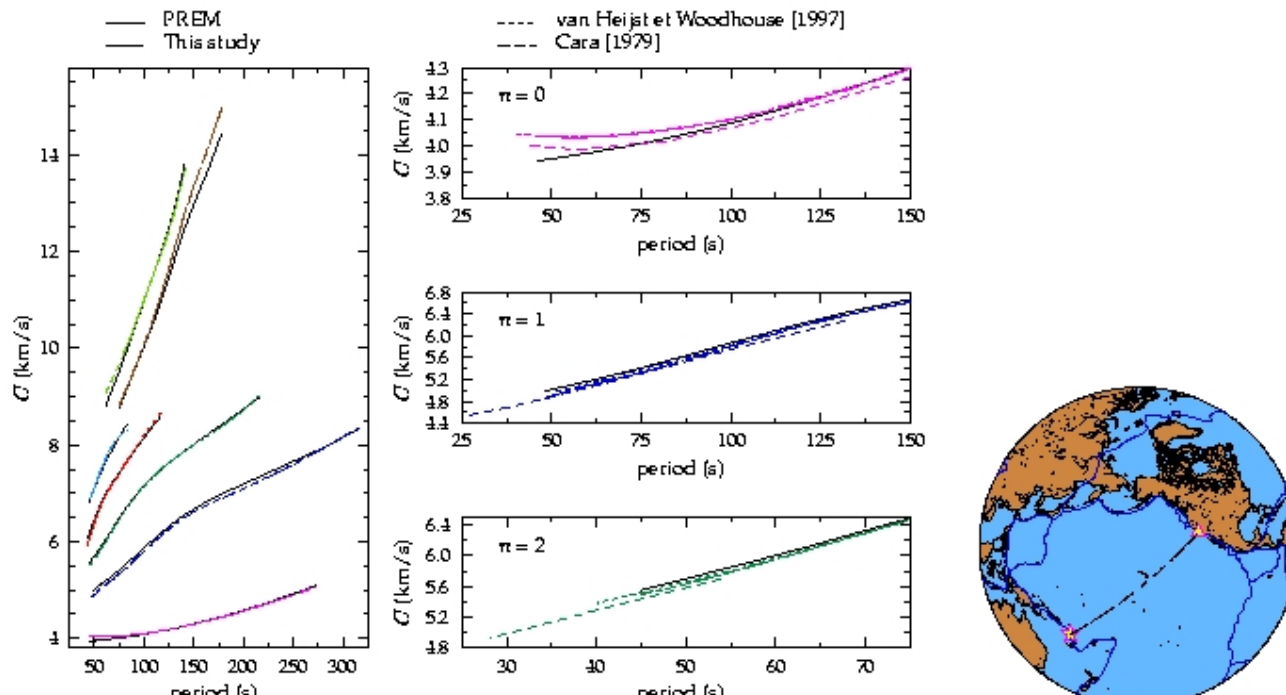


Continuous parameterization



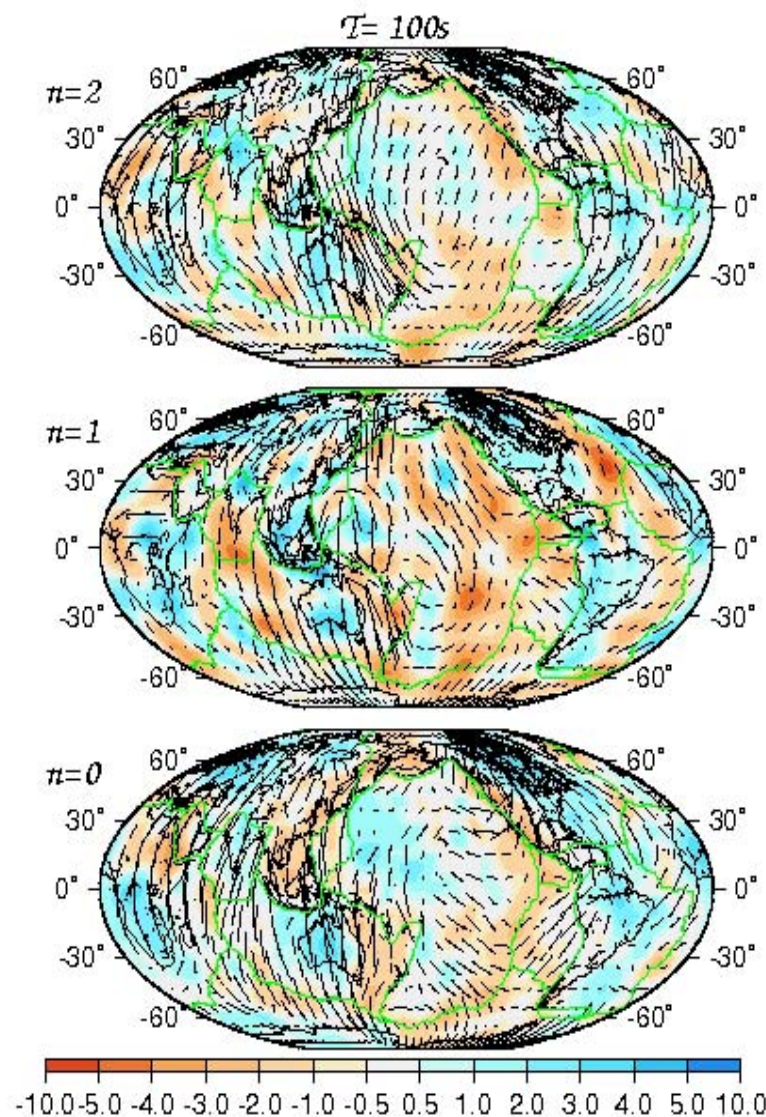
- Spherical harmonic expansion
- Lateral resolution:
Hor 1000km, Rad 50km => $500 * 60 * 14 \approx 420,000$ parameters

Calculation of dispersion curves: Fundamental modes and higher modes



Beucler et al., 2002

Phase velocity maps At 100s



2nd overtone

1st overtone

Fundamental mode

Beucler and Montagner, 2006

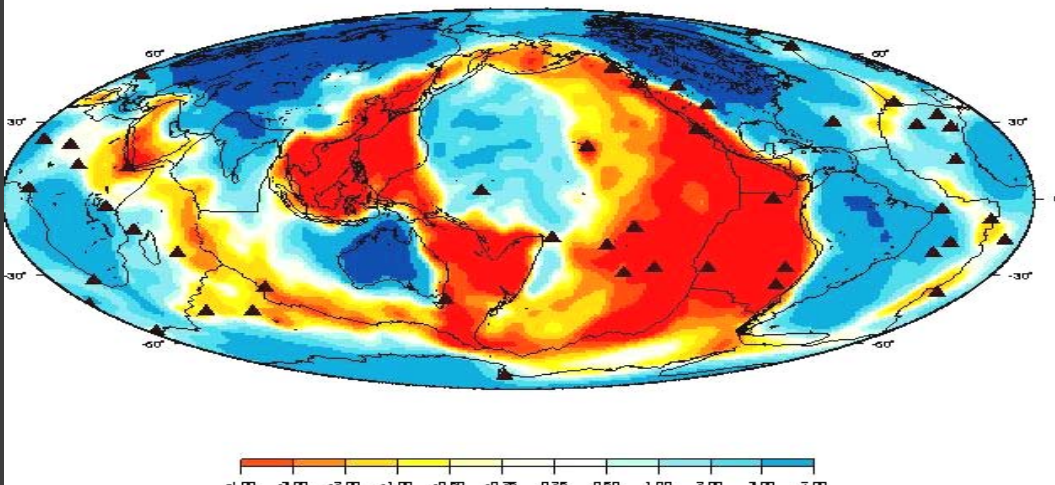
Global Tomography

Scale $\Lambda \approx 2000\text{km}$ (degree 20)

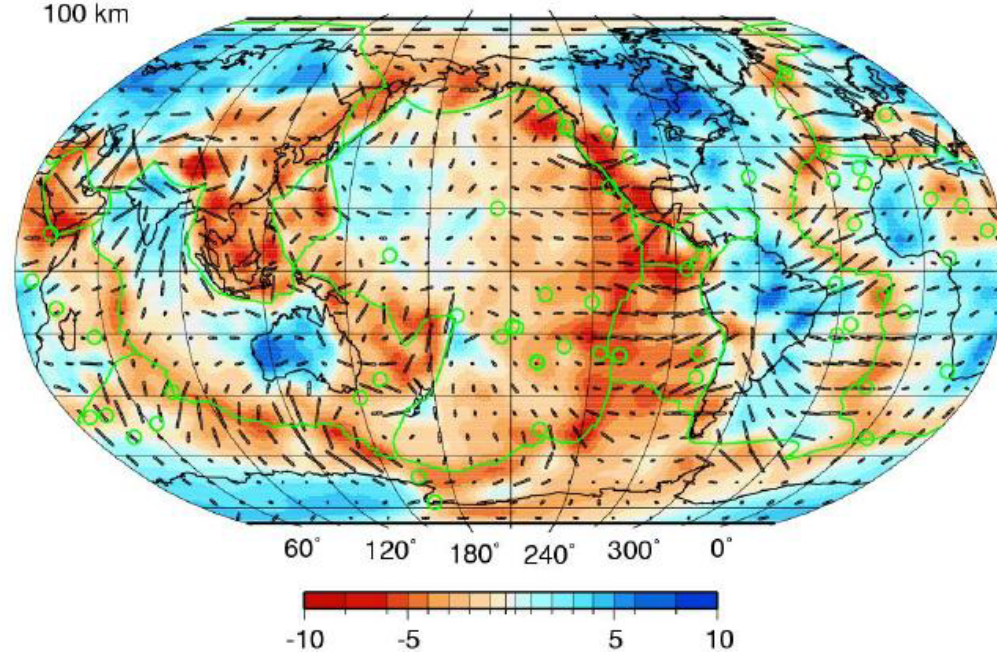
Seismic wavelength $\lambda \leq 500\text{km}$

→ Ray theory applies

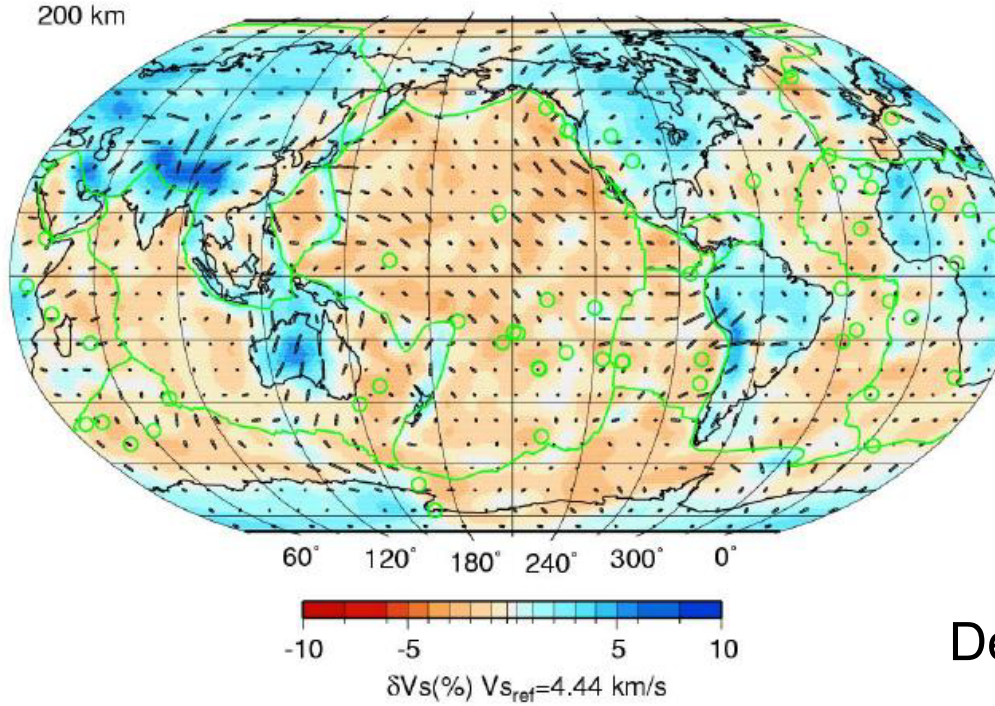
Shear wave velocities - depth = 100km



100 km



200 km

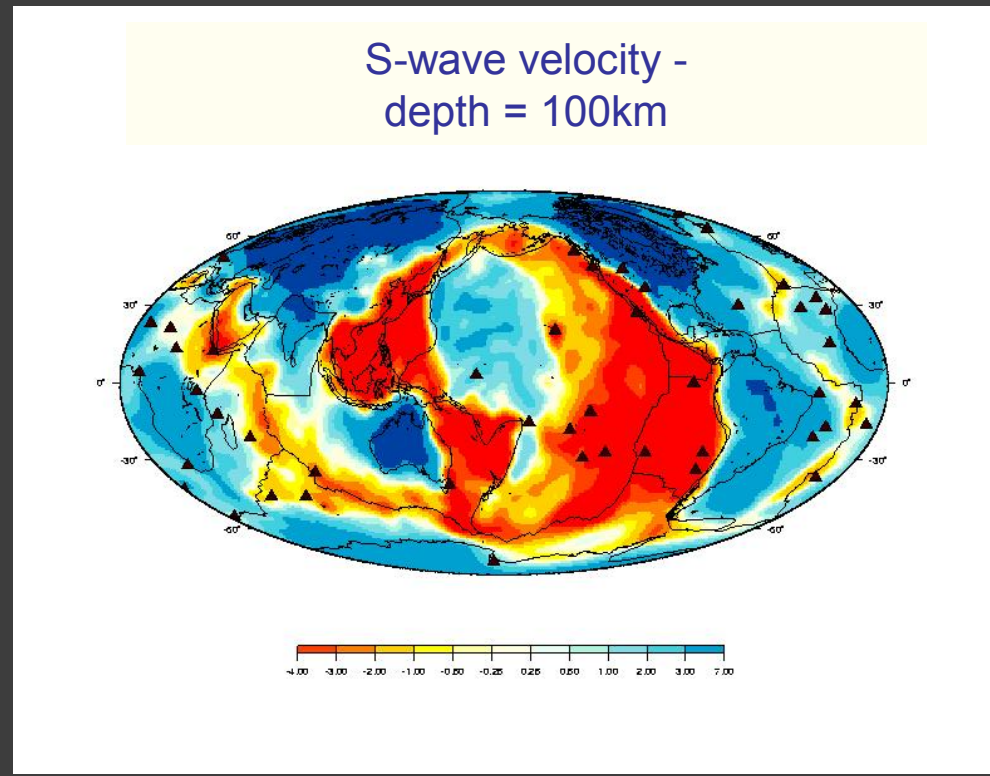


Debayle et al., 2005

CAN WE NEGLECT SMALL-SCALE HETEROGENEITIES?

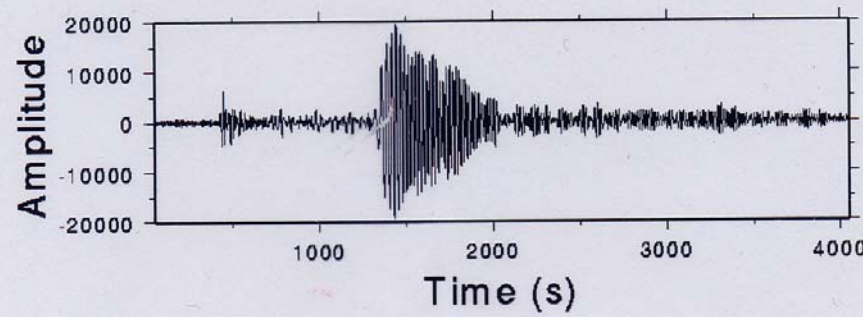
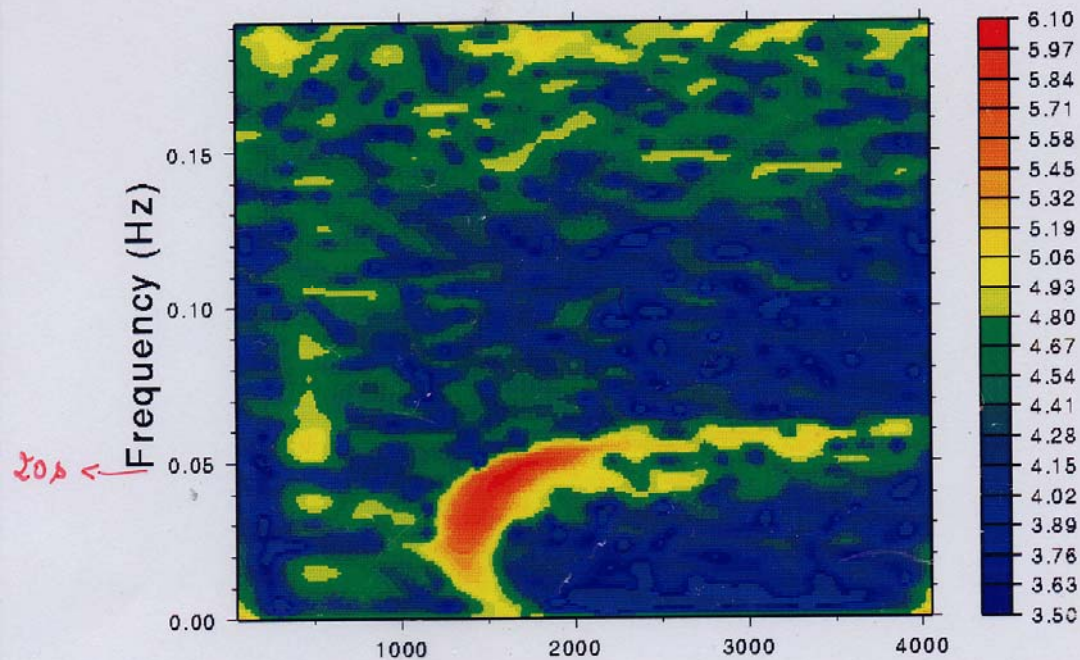
Scale $\Lambda > 1000\text{km}$

Seismic wavelength $20\text{km} \leq \lambda \leq 500\text{km}$



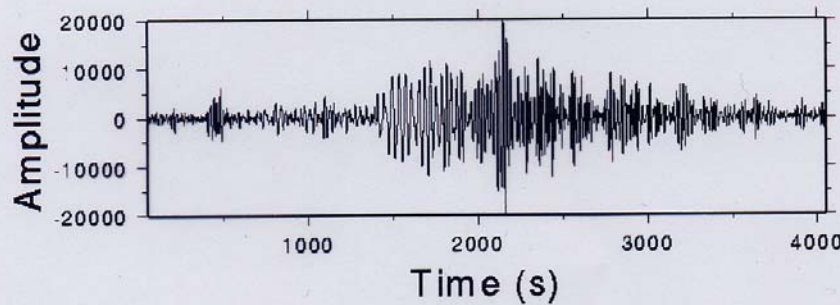
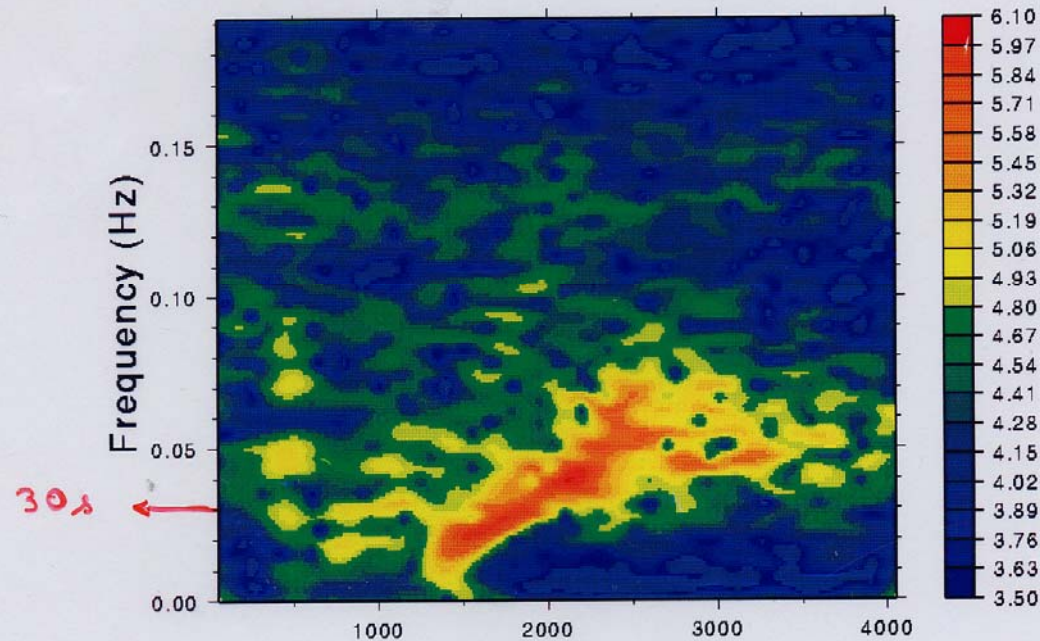
Spectrogram at station PPT (Z component, distance=82 degrees)

Aleutians 1992/03/02 depth=39km m.s=6.8



Spectrogram at station SSB (Z component, distance=80 degrees)

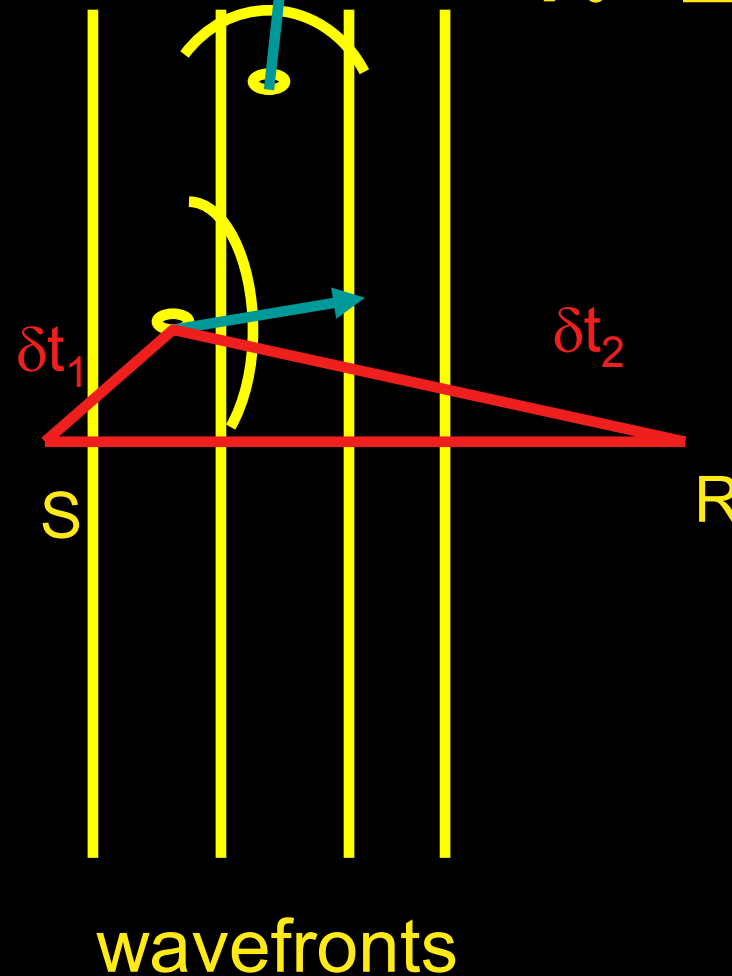
Aleutians 1992/03/02 depth=39km m s=6.8



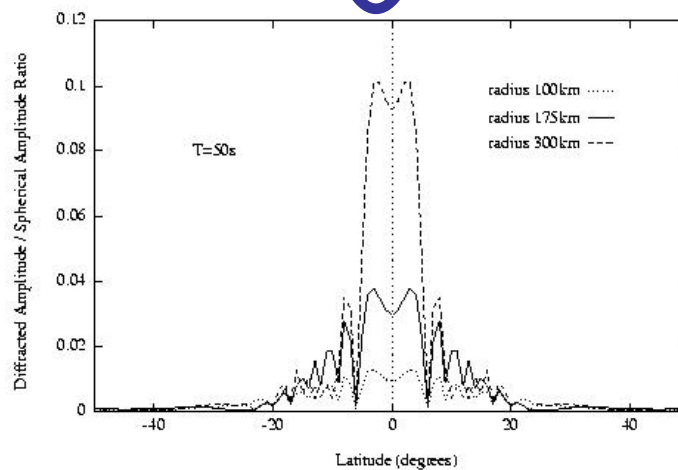
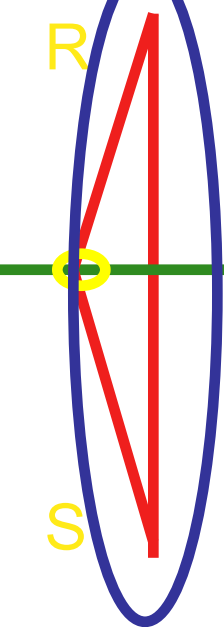
Λ heterogeneity scale, λ wavelength

Diffracted waves

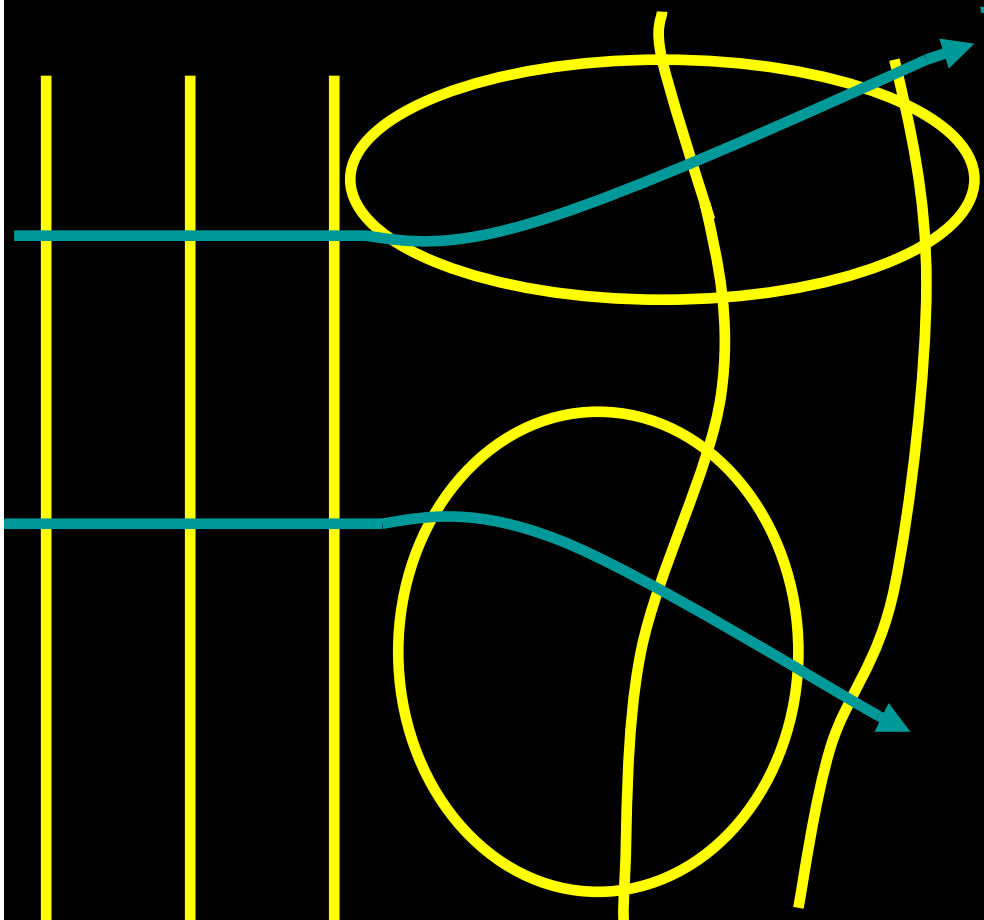
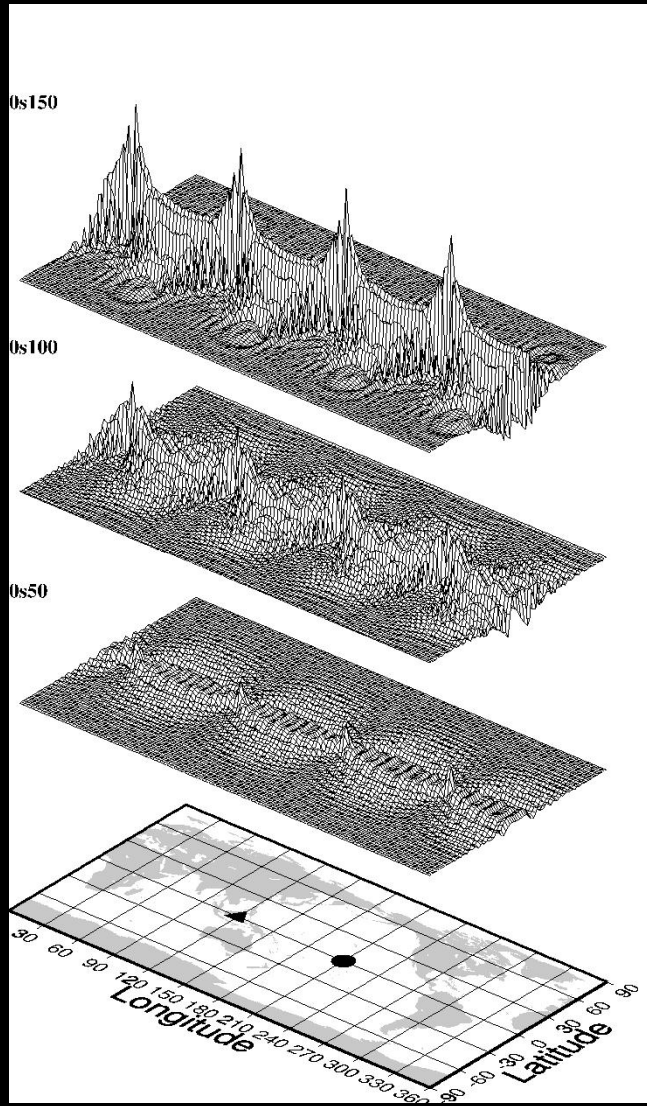
$\lambda \sim$  Λ or $\lambda \gg \Lambda$



$$\delta t_1 + \delta t_2 = \text{cst}$$



Λ heterogeneity scale, λ wavelength



$$\lambda \ll \Lambda$$

Typical scales $\Lambda \approx 2,000\text{km}$, $\lambda \approx 500\text{km}$

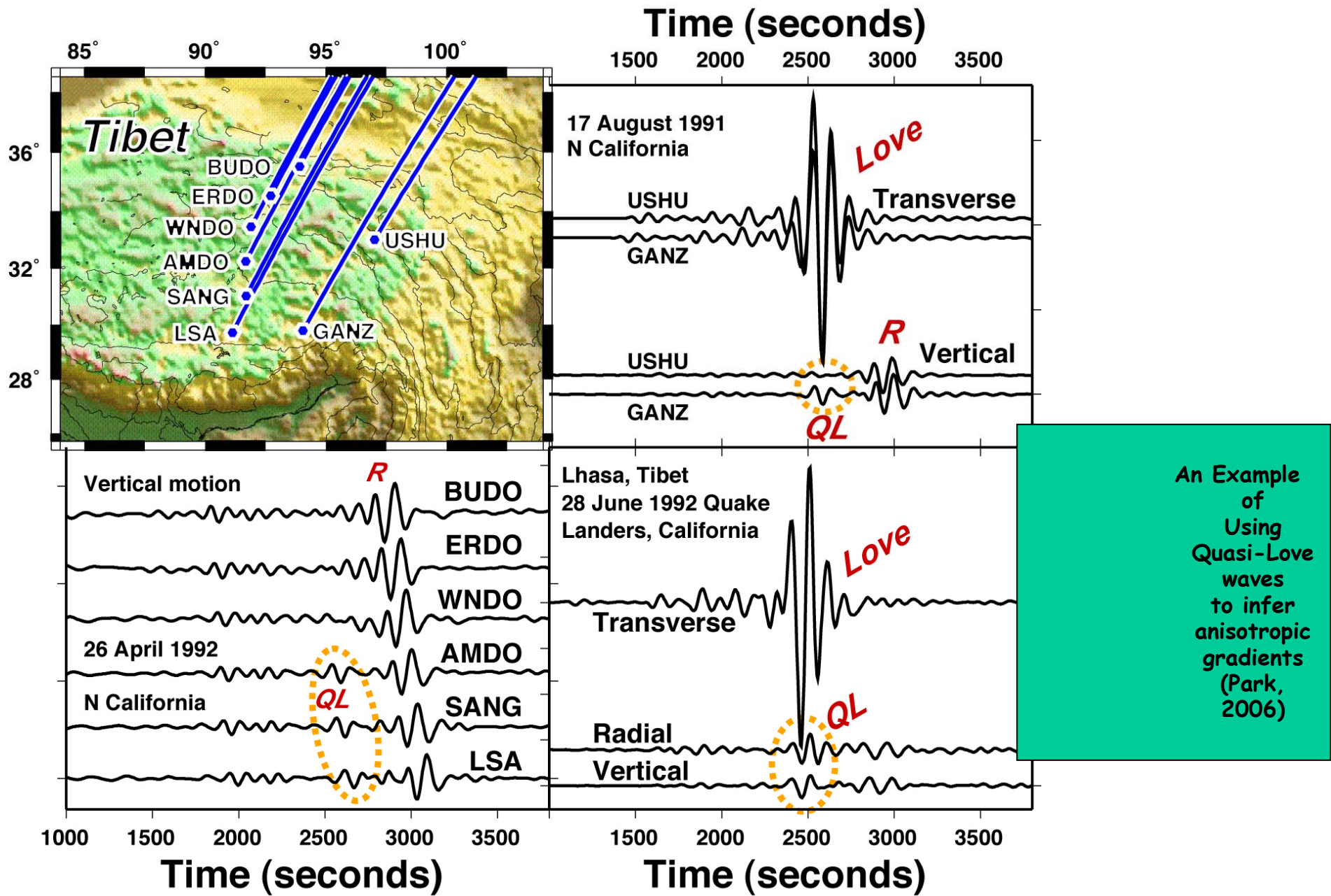
Finite frequency sensitivity of surface waves to anisotropy using adjoint methods

Anne Sieminski¹, Qinya Liu², Jeannot Trampert¹
and Jeroen Tromp²

- (1) Utrecht University
- (2) Caltech Seismological Lab

Effects on amplitude?

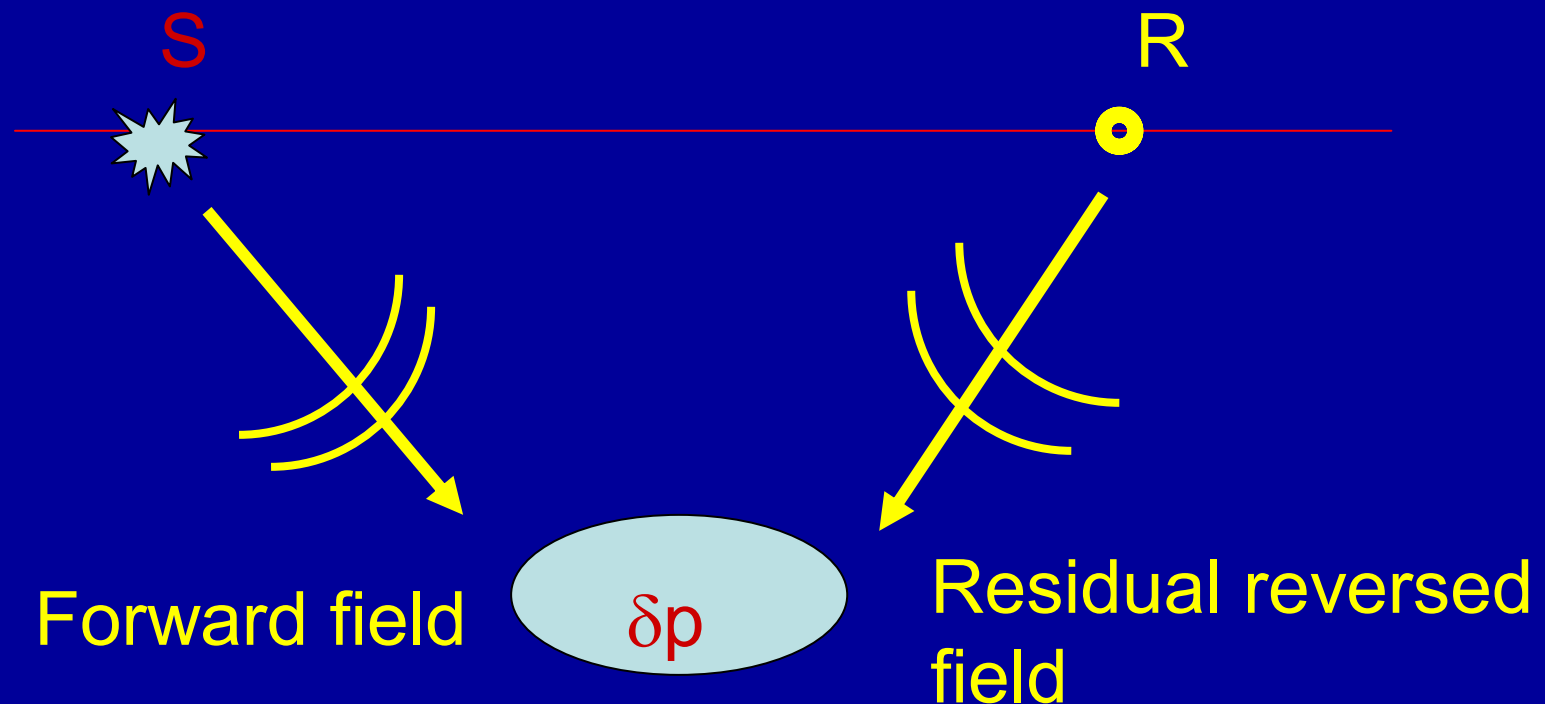
- Surface wave tomography of mantle anisotropy is based on ray theory
- Finite frequency tomography has been tested to improve the imaging of the isotropic mantle
- How do finite frequency surface waves "sense" anisotropy ?
- Computational tool : Adjoint Spectral Element Method (ASEM) (Tromp et al., 2005)



Time Reversal- Adjoint Method

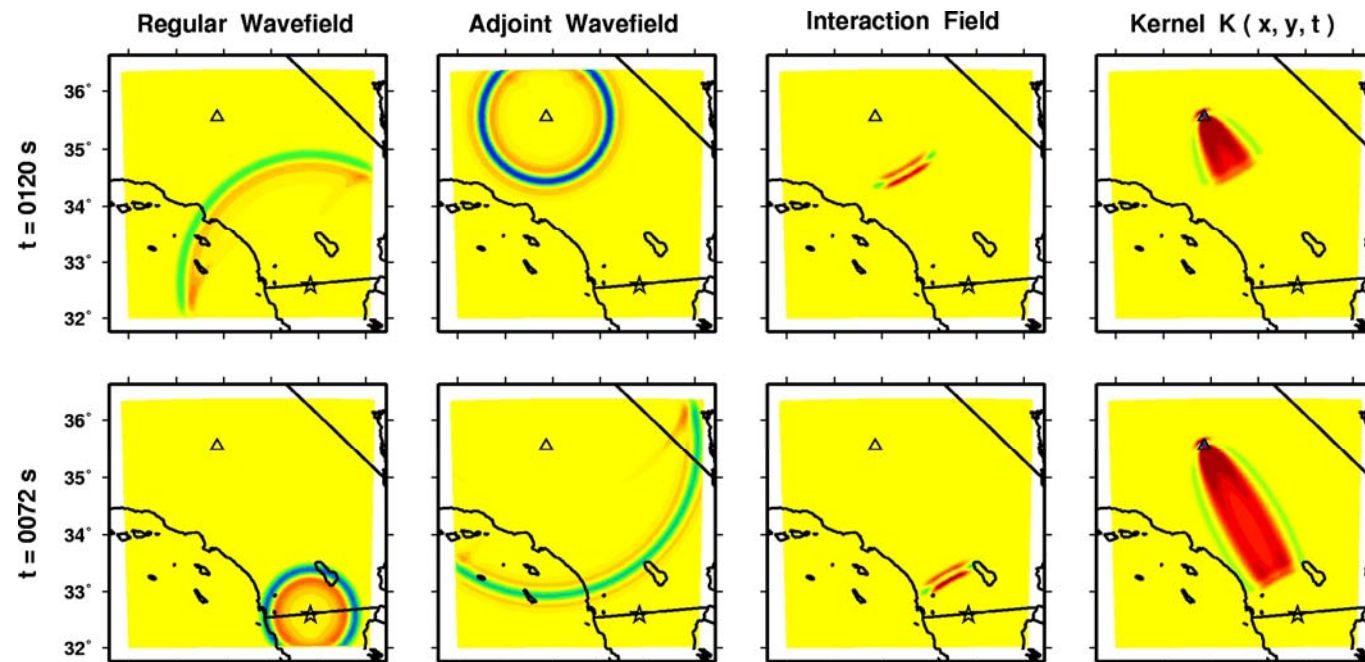
(Tarantola, 1984, Tromp et al., 2005):

Adjoint => Fréchet Derivatives



Sensitivity computation (1)

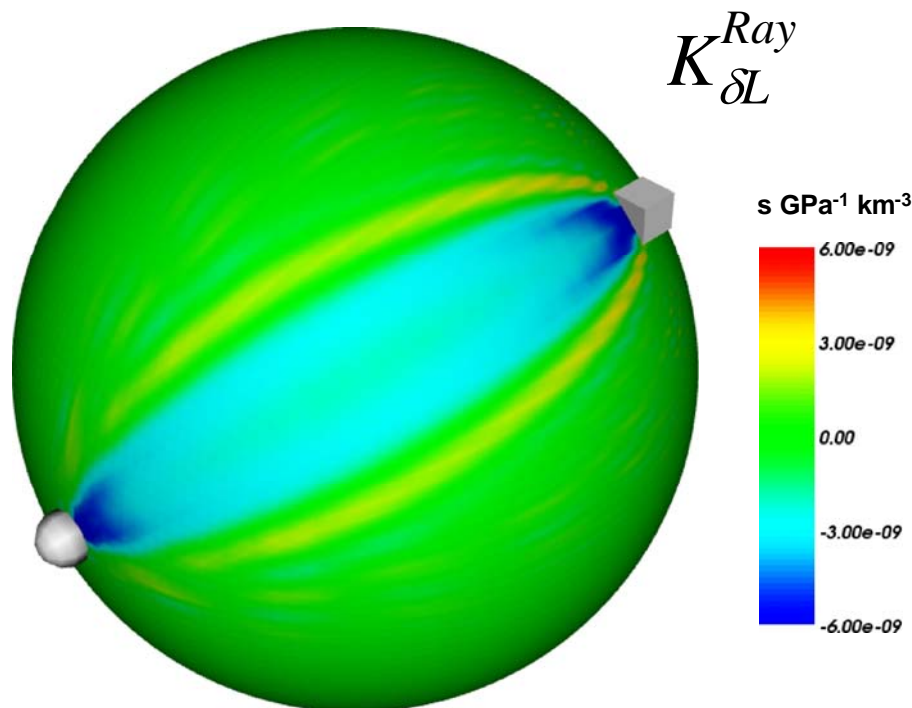
- Sensitivity kernel : $\delta T = \iiint K_{\delta m}^{\delta T}(x) \delta m(x) dx^3$
- Construction :



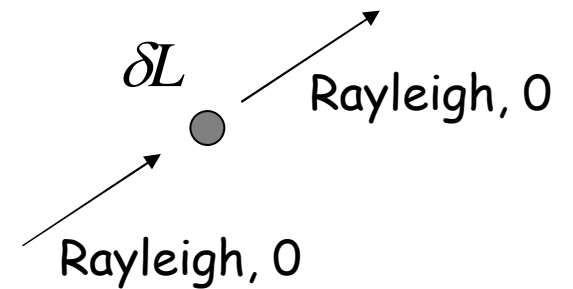
Tape et al. (2006)

Sensitivity kernels (2)

- Off the ray path :



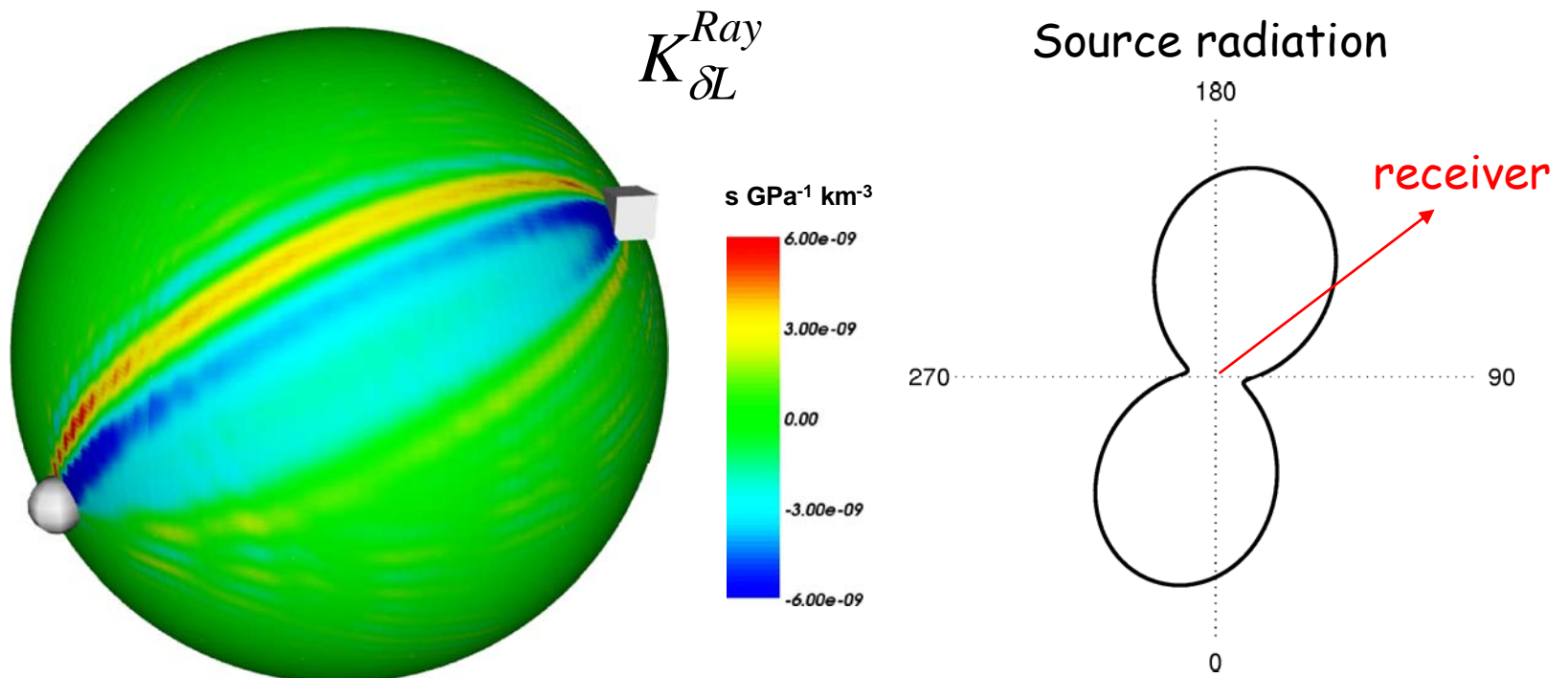
Interpretation with
Born scattering theory



at 150 km depth (mode 0 ; $100s < T < 180s$; $\Delta = 120^\circ$)

Sensitivity kernels (3)

- Off the ray path :

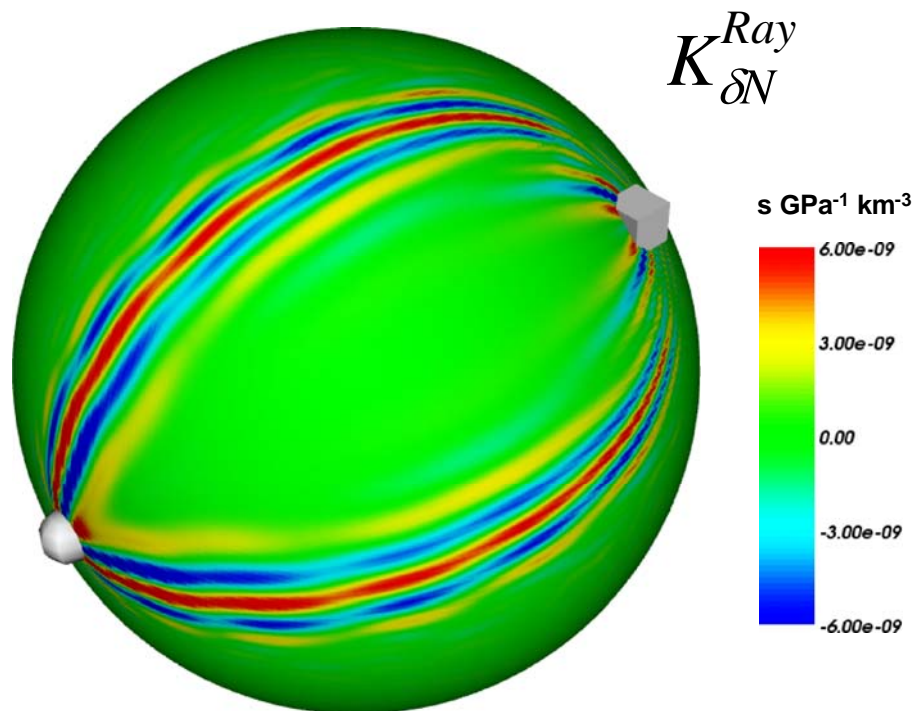


at 150 km depth (mode 0 ; $100s < T < 180s$; $\Delta = 120^\circ$)

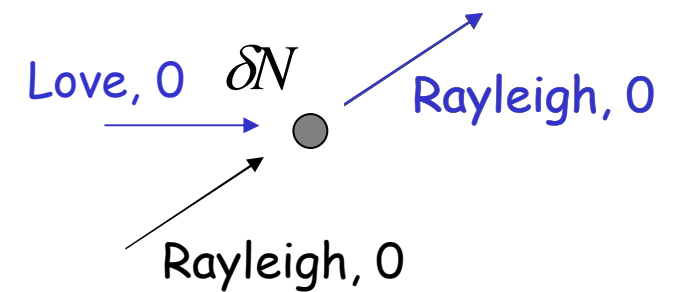
Sensitivity kernels

(4)

- Love-Rayleigh coupling effect :



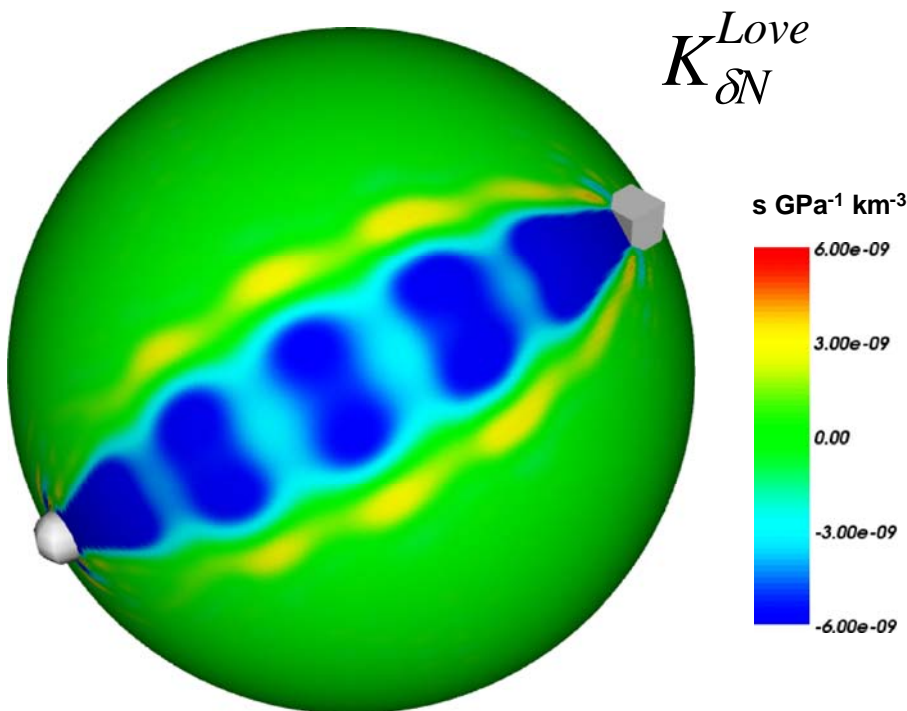
Interpretation with
Born scattering theory



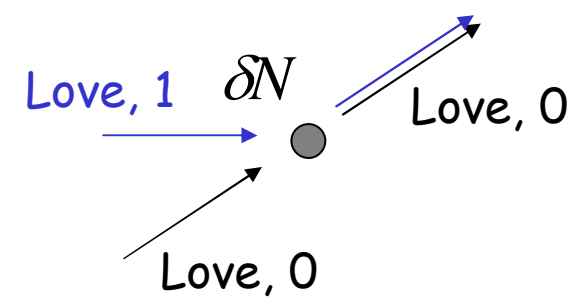
at the surface (mode 0 ; $100s < T < 180s$; $\Delta = 120^\circ$)

Sensitivity kernels (5)

- Cross-branch coupling effect :



Interpretation with
Born scattering theory



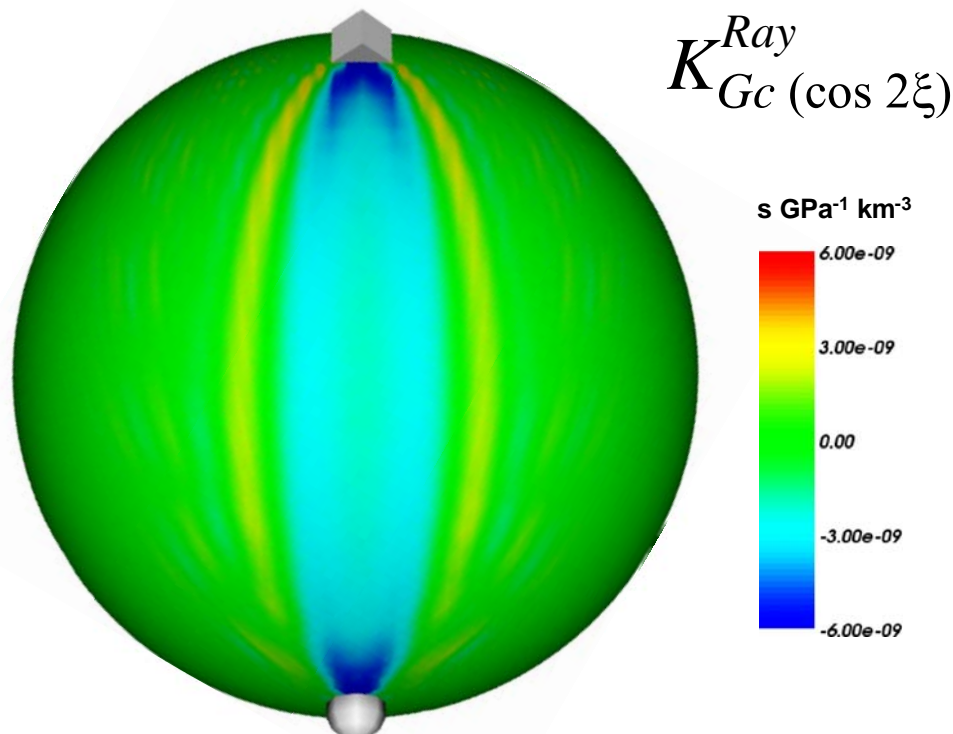
at the surface (mode 0 ; $100s < T < 180s$; $\Delta = 120^\circ$)



Sensitivity kernels

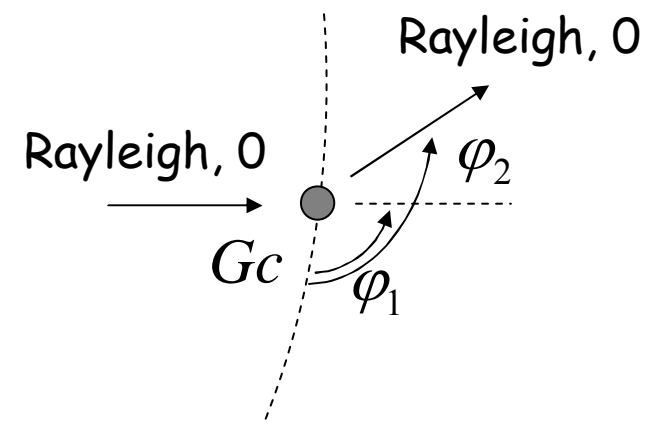
(6)

- Path-dependency (azimuthal anisotropy) :



In Born scattering theory

$$K_{Gc}^{Ray} \sim \cos(\varphi_1 + \varphi_2)$$

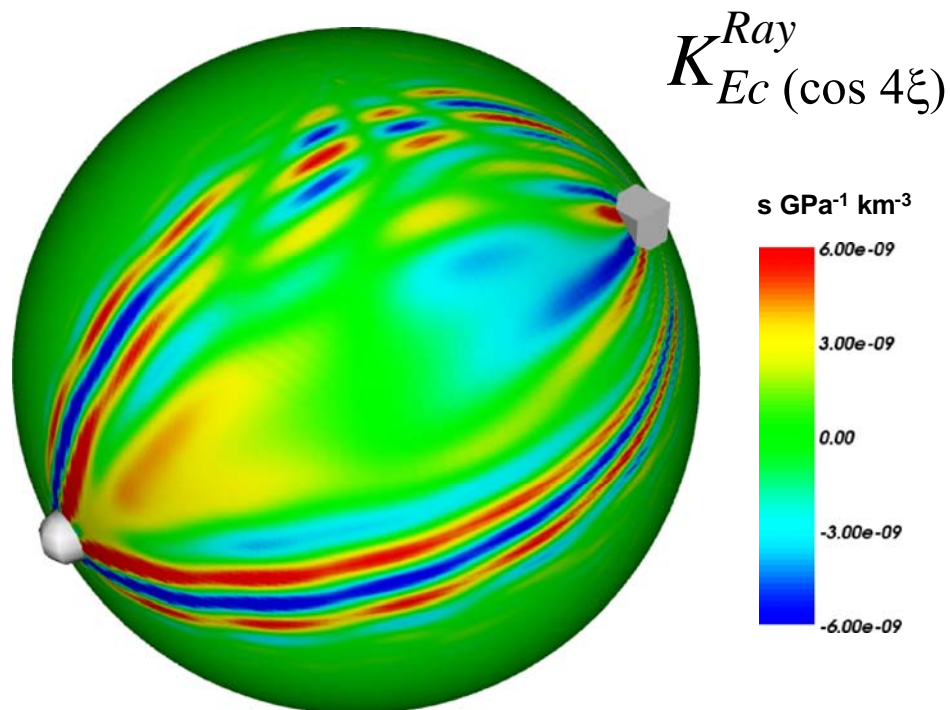


at the surface (mode 0 ; $100\text{s} < T < 180\text{s}$; $\Delta = 120^\circ$)



Sensitivity kernels (7)

- Love-Rayleigh coupling and path-dependency :



at the surface (mode 0 ; $100s < T < 180s$; $\Delta = 120^\circ$)



Conclusion

- Surface wave amplitude sensitivity to anisotropy is controlled by :
 - significant mode coupling effects
 - strong path-dependency (azimuthal anisotropy)
 - source radiation
- ⇒ Most of the sensitivity kernels do not show a simple elliptical pattern
- ⇒ Consequences for tomography ?